Evaluation of ground-based black carbon measurements by filter-based photometers at two Arctic sites

DOI:
10.1002/2016JD025843

Document Version
Final published version

AGU PUBLICATIONS

JGR

Journal of Geophysical Research: Atmospheres

RESEARCH ARTICLE

10.1002/2016JD025843

Key Points:

- We evaluated the accuracy of black carbon (BC) measurements at Barrow, Alaska, and Ny-Ålesund, Spitsbergen, in the Arctic
- At Barrow, seasonally averaged BC mass concentrations decreased in winter and summer at a rate of $0.55 \pm 0.30\ \mathrm{ng\ m^{-3}\ yr^{-1}}$ during 1998–2015
- We established seasonal variations of BC at the two sites and evaluated the causes of the inconsistency of the previously reported data

Correspondence to:
Y. Kondo,
kondo.yutaka@nipr.ac.jp

Citation:
Sinha, P. R., et al. (2017), Evaluation of ground-based black carbon measurements by filter-based photometers at two Arctic sites, *J. Geophys. Res. Atmos.*, *122*, 3544–3572, doi:10.1002/2016JD025843.

Received 26 AUG 2016
Accepted 3 MAR 2017
Accepted article online 9 MAR 2017
Published online 29 MAR 2017

Evaluation of ground-based black carbon measurements by filter-based photometers at two Arctic sites

P. R. Sinha[1,2], Y. Kondo[3], M. Koike[1], J. A. Ogren[4,5], A. Jefferson[5], T. E. Barrett[6], R. J. Sheesley[6,7], S. Ohata[1], N. Moteki[1], H. Coe[8], D. Liu[8], M. Irwin[9], P. Tunved[10], P. K. Quinn[11], and Y. Zhao[12]

[1]Department of Earth and Planetary Science, Graduate School of Science, University of Tokyo, Tokyo, Japan, [2]Balloon Facility, Tata Institute of Fundamental Research, Hyderabad, India, [3]National Institute of Polar Research, Tachikawa, Japan, [4]NOAA/ESRL Global Monitoring Division, Boulder, Colorado, USA, [5]Cooperative Institute for Research in Environmental Sciences, University of Colorado Boulder, Boulder, Colorado, USA, [6]The Institute of Ecological, Earth, and Environmental Sciences, Baylor University, Waco, Texas, USA, [7]Department of Environmental Science, Baylor University, Waco, Texas, USA, [8]Centre for Atmospheric Science, School of Earth, Atmospheric and Environmental Sciences, University of Manchester, Manchester, UK, [9]Cambustion Ltd, Cambridge, UK, [10]Department of Environmental Science and Analytical Chemistry, Stockholm University, Stockholm, Sweden, [11]NOAA PMEL, Seattle, Washington, USA, [12]Air Quality Research Center, University of California, Davis, California, USA

Abstract Long-term measurements of the light absorption coefficient (b_{abs}) obtained with a particle soot absorption photometer (PSAP), b_{abs} (PSAP), have been previously reported for Barrow, Alaska, and Ny-Ålesund, Spitsbergen, in the Arctic. However, the effects on b_{abs} of other aerosol chemical species coexisting with black carbon (BC) have not been critically evaluated. Furthermore, different mass absorption cross section (MAC) values have been used to convert b_{abs} to BC mass concentration ($M_{BC} = b_{abs}/\mathrm{MAC}$). We used a continuous soot monitoring system (COSMOS), which uses a heated inlet to remove volatile aerosol compounds, to measure b_{abs} (b_{abs} (COSMOS)) at these sites during 2012–2015. Field measurements and laboratory experiments have suggested that b_{abs} (COSMOS) is affected by about 9% on average by sea-salt aerosols. M_{BC} values derived by COSMOS (M_{BC} (COSMOS)) using a MAC value obtained by our previous studies agreed to within 9% with elemental carbon concentrations at Barrow measured over 11 months. b_{abs} (PSAP) was higher than b_{abs} (COSMOS), by 22% at Barrow (PM_1) and by 43% at Ny-Ålesund (PM_{10}), presumably due to the contribution of volatile aerosol species to b_{abs} (PSAP). Using b_{abs} (COSMOS) as a reference, we derived M_{BC} (PSAP) from b_{abs} (PSAP) measured since 1998. We also established the seasonal variations of M_{BC} at these sites. Seasonally averaged M_{BC} (PSAP) decreased at a rate of about $0.55 \pm 0.30\ \mathrm{ng\ m^{-3}\ yr^{-1}}$. We also compared M_{BC} (COSMOS) and scaled M_{BC} (PSAP) values with previously reported data and evaluated the degree of inconsistency in the previous data.

1. Introduction

Black carbon (BC) particles are emitted as a result of incomplete combustion of both natural and anthropogenic carbon-based fuels. BC particles influence the radiation budget of the Earth's atmosphere by strongly absorbing solar radiation [*Bond et al.*, 2013; *Kondo*, 2015]. Warming is occurring in the Arctic at about twice the global average rate [*Shindell and Faluvegi*, 2009] owing to a combination of climate feedbacks, including radiation feedback [*Sand et al.*, 2016]. Light-absorbing particles such as BC likely contribute to radiative forcing in the Arctic also by changing the albedo of snow through the deposition of BC [*Bond et al.*, 2013; *Flanner et al.*, 2007; *Shindell and Faluvegi*, 2009]. However, estimates by climate models of the effects of BC on Arctic warming are still highly uncertain, in part because measurements of the spatiotemporal distribution of the mass concentration of BC (M_{BC}) in the atmosphere are limited and not sufficiently accurate.

To better understand the distribution of M_{BC} and the processes controlling M_{BC} in the Arctic, both aircraft measurements [*Kondo et al.*, 2011a; *Liu et al.*, 2015; *Matsui et al.*, 2011; *McNaughton et al.*, 2011; *Spackman et al.*, 2010; *Warneke et al.*, 2009, 2010] and ground-based measurements [*Bodhaine*, 1995; *Delene and Ogren*, 2002; *Eleftheriadis et al.*, 2009; *Hirdman et al.*, 2010a; *Sharma et al.*, 2013] have been conducted. We summarize the nomenclature of physical parameters related to absorption and scattering by aerosol particles and the mass concentration of BC particles derived by different instruments in Table 1.

Table 1. Summary of the Variable Symbols and Acronyms Used in This Study

Term	Definition
b_{abs}	Aerosol light absorption coefficient, also denoted as σ_{ap} in the literature
b_{sca}	Aerosol light-scattering coefficient, also denoted as σ_{sp} in the literature
b_{abs} (COSMOS)	b_{abs} measured by a continuous soot monitoring system (COSMOS)
b_{abs} (PSAP)	b_{abs} measured by a particle soot absorption photometer (PSAP) or continuous light absorption photometer (CLAP)
MAC	Mass absorption cross section
M_{BC}	Mass concentration of black carbon (BC). Used in a general sense, and not used when reporting or discussing measurements of the mass concentration of BC
M_{BC} (COSMOS)	Mass concentration of black carbon derived from measurements of the light absorption coefficient (b_{abs}) with COSMOS using a MAC of 8.73 $m^2\,g^{-1}$
M_{BC} (PSAP)	Mass concentration of black carbon derived from b_{abs} (PSAP) by using a MAC value of 10.6 $m^2\,g^{-1}$ at Barrow and 12.5 $m^2\,g^{-1}$ at Ny-Ålesund, as derived herein such that the average M_{BC} (PSAP) values agree with M_{BC} (COSMOS) values. Termed equivalent black carbon (EBC) by *Petzold et al.* [2013]
M_{BC}^* (PSAP-PM_1)	M_{BC} (PSAP) for PM_1 derived by *Hirdman et al.* [2010a, 2010b] by using a MAC of 10 $m^2\,g^{-1}$
M_{BC}^* (PSAP-PM_{10})	M_{BC} (PSAP) for PM_{10} derived by *Hirdman et al.* [2010a, 2010b] by using a MAC of 10 $m^2\,g^{-1}$
M_{BC} (aethalometer)	M_{BC} derived from measurements of b_{abs} with an aethelometer by *Sharma et al.* [2013]
M_{BC} (SP2)	Mass concentration of refractory black carbon (rBC) derived from measurements with a single particle soot photometer (SP2)
M_{EC}	Mass concentration of elemental carbon (EC) derived from thermo-optical transmittance (TOT) measurements of evolved carbon from filter samples

Detailed studies of emissions of BC from different sources (e.g., Asia, Europe, and North America) and its subsequent transport in the planetary boundary layer and free troposphere have been made by using aircraft measurements [*Brock et al.*, 2011; *Kondo et al.*, 2011a; *Liu et al.*, 2015; *Sahu et al.*, 2012; *Spackman et al.*, 2010; *Warneke et al.*, 2009, 2010]. These studies used a single particle soot photometer (SP2) and obtained accurate measurements of BC size distributions [e.g., *Schwarz et al.*, 2006; *Moteki and Kondo*, 2008]. However, aircraft measurements are limited both spatially and temporally.

To date, most autonomous and continuous measurements of M_{BC} in the Arctic region have been made by a filter-based optical technique, mainly with a particle soot absorption photometer (PSAP; Radiance Research, Seattle, WA) or an aethalometer (Magee Scientific, Berkeley, CA, USA) [*Bodhaine*, 1995; *Delene and Ogren*, 2002; *Eleftheriadis et al.*, 2009; *Sharma et al.*, 2013]. However, these studies did not perform detailed error analyses, so the accuracy of the M_{BC} values derived from those measurements is uncertain.

Measurements obtained by filter-based absorption techniques need to be corrected for the effects of coexisting non-BC aerosol particles in the filter medium because ambient aerosols comprise a complex mixture of light-absorbing and nonabsorbing particles which optically interact [*Bond et al.*, 1999, 2013]. We have deployed a continuous soot monitoring system called continuous soot monitoring system (COSMOS) (Kanomax, Osaka, Japan) [*Miyazaki et al.*, 2008; *Kondo et al.*, 2009, 2011b], which is a filter-based instrument equipped with an inlet heated at 300°C to remove nonrefractory components from the aerosol phase.

However, light transmission through the filter matrix is reduced not only due to refractory absorbing particles but also due to the presence of embedded light-scattering particles that do not evaporate during sampling through the heated inlet. As a result, M_{BC} determined by COSMOS (M_{BC} (COSMOS)) may be overestimated, though *Verma et al.* [2011] found this effect to be small in Asia. Near the surface in the Arctic, however, M_{BC} is often lower by an order of magnitude than it is in midlatitudes [e.g., *Liu et al.*, 2015; *Spackman et al.*, 2010]. Therefore, nonvolatile aerosol components such as sea salt and mineral dust particles may substantially interfere with the M_{BC} (COSMOS) measurements, depending on their concentrations relative to those of BC. Thus, there is a strong need to evaluate the uncertainties of M_{BC} (COSMOS), especially in remote regions such as the Arctic.

For this purpose, we conducted laboratory experiments to estimate how the presence of sea-salt particles affected M_{BC} (COSMOS). For overall evaluation of the accuracy of M_{BC} (COSMOS), we compared M_{BC} (COSMOS) with measurements of the mass concentration of elemental carbon (EC) (M_{EC}) made by the thermal-optical transmittance (TOT) technique at Barrow. We also compared M_{BC} (COSMOS) with M_{BC} measured near Ny-Ålesund by an SP2 onboard aircraft, although the available aircraft data are limited. We used the results of these comparisons to investigate the correlation of the M_{BC} (COSMOS) values with absorption coefficients measured by a PSAP (b_{abs} (PSAP)) operated at Barrow, Alaska (71.32°N, 156.61°E, 10 m above sea level), by the National Oceanic and Atmospheric Administration (NOAA) Earth System Research Laboratory, Global Monitoring Division and at Zeppelin Station (78.92°N, 11.93°E, 474 m above sea level), Ny-Ålesund, Spitsbergen, operated by the Norwegian Polar Institute. We then scaled b_{abs} (PSAP) measured at Barrow and Ny-Ålesund by comparing them with M_{BC} (COSMOS) based on high correlations between PSAP and COSMOS measurements. Finally, we used the scaled PSAP measurements to derive the long-term variations of M_{BC} (PSAP) at these sites.

2. Absorption Coefficients and M_{BC} Obtained by PSAP and COSMOS

The principles of operation of PSAP and COSMOS are identical; the attenuation of light at a given wavelength λ, $b_0(\lambda)$, in a filter-based absorption photometer, is determined by the following equation:

$$b_0(\lambda) = \frac{A}{V_a} \ln\left[\frac{I_{t-\Delta t}}{I_t}\right], \quad (1)$$

where A is the area of the sample spot, V_a is the air sample volume during a given time period between $(t - \Delta t)$ and t, and $I_{t-\Delta t}$ and I_t are the average transmittances at $(t - \Delta t)$ and t, respectively [*Bond et al.*, 1999].

In the case of a PSAP, absorption coefficients of aerosol particles collected on filters (b_{abs}) are derived from the measured attenuation b_0. Because the b_0 values measured by this instrument are influenced by light scattering by aerosols, these contributions are corrected by applying the empirical relation of *Bond et al.* [1999]:

$$b_{abs}(\text{PSAP}) = f_{fil} b_0 - f_{sca} b_{sca}, \quad (2)$$

where the second term on the right-hand side, $f_{sca}b_{sca}$, represents a correction for light scattering by aerosol particles collected on filters. b_{sca} is obtained by independent measurements, such as with a nephelometer. For PSAPs, f_{sca} has been estimated to be 0.016 ± 0.016 [*Bond et al.*, 1999]. In equation (2), f_{fil} represents the increase in absorption by multiple scattering in the filter medium. In this study, the following equation, which was derived by using polydisperse nigrosine particles, is used for f_{fil} [*Bond et al.*, 1999]:

$$f_{fil}(\text{Tr}) = \frac{1}{[1.0796 \ \text{Tr} + 0.71]B} \quad \text{for Tr} \geq 0.7, \quad (3)$$

where Tr ($=I_t/I_{t=0}$) is the filter transmission and $B = 1.397$ is a scaling factor [*Bond et al.*, 1999; *Ogren*, 2010]. Consequently, non-BC light-scattering particles (LSPs) can affect the estimate of b_{abs} of BC in PSAP measurements, and the error associated with the correction for non-BC LSPs can be large, depending on the relative magnitudes of the two terms on the right-hand side of equation (2) [*Bond et al.*, 1999].

For COSMOS, b_{sca} is very close to zero for most aerosols, owing to the use of the heated inlet to remove volatile non-BC species [*Kondo et al.*, 2011b]. In fact, the contribution of the $f_{sca}b_{sca}$ term of equation (2) to b_{abs} (COSMOS) values has been estimated to be about 2% at midlatitudes [*Kondo*, 2015]. Hence, we used the following equation for COSMOS:

$$b_{abs}(\text{COSMOS}) = f_{fil} b_0. \quad (4)$$

Equation (3) was used to account for the effect of multiple scattering for COSMOS. As a result of the removal of volatile non-BC species, errors associated with non-BC LSPs are small and COSMOS measures b_{abs} of bare BC particles (core BC particles) accurately when all scattering particles are volatile. In contrast, a PSAP measures the light absorption of all particles, which is possibly enhanced by volatile coatings on the BC particles (discussed below) and by scattering from nonrefractory particles within the PSAP filter matrix.

Changes in soot morphology during heating do not substantially affect b_{abs} measurements by the COSMOS instrument. Laboratory experiments with an SP2 have shown that the change in the diameter of fullerene soot with initial diameters of 150 and 320 nm caused by heating the soot to 300°C is about 3% [*Irwin et al.*, 2013]. Characteristics of fullerene soot were found to be representative of the ambient BC in Tokyo [*Moteki and Kondo*, 2010]. A PSAP measures the light absorption of all particles, which is possibly enhanced by coatings on BC particles, as discussed below.

With both PSAPs and COSMOS, M_{BC} (g m^{-3}) can be estimated by dividing b_{abs} (m^{-1}) by the mass absorption cross section of BC (MAC) (m^2 g^{-1}), if the effects of LSPs are corrected for with sufficient accuracy and the effect of light-absorbing particles other than BC is neglected. Namely,

$$M_{BC} = b_{abs}/\mathrm{MAC}. \tag{5}$$

Under the assumptions mentioned above, b_{abs} (COSMOS) corresponds to the absorption of bare BC particles, so MAC (COSMOS) depends only (and slightly) on the size distribution of bare BC particles [*Kondo et al.*, 2011b]. On the other hand, b_{abs} values obtained by PSAP potentially depend on the mixing state of BC and are also sensitive to absorption by non-BC species, such as brown carbon, which COSMOS does not sense. They also depend on the BC size distribution.

Light absorption by BC particles is enhanced by coatings of non-BC compounds, the so-called lens effect [e.g., *Shiraiwa et al.*, 2010; *Bond et al.*, 2013]. Therefore, the MAC (PSAP) value used to calculate M_{BC} (PSAP) should be varied according to the mixing state of BC. In other words, the use of a constant MAC (PSAP) value to derive M_{BC} (PSAP) under varying atmospheric environmental conditions will introduce additional uncertainties into M_{BC} (PSAP) estimates.

To summarize, in principle, COSMOS measures b_{abs} of bare BC particles accurately, whereas PSAP measures b_{abs} of all particles, and the measured value is enhanced by coatings on BC particles. Furthermore, the MAC value used with COSMOS (MAC of bare BC particles) has less uncertainty than that used with PSAPs (MAC of various BC mixing states). Therefore, M_{BC} (COSMOS) is considered to be more accurate than M_{BC} (PSAP).

We note that M_{BC} (COSMOS) can be influenced not only by the uncertainty of MAC (COSMOS) due to variability of the BC size distribution but also by refractory LSPs (such as sea-salt and dust particles). These uncertainties are examined individually in the following sections. We then compare M_{BC} (COSMOS) values with M_{BC} (PSAP) values and discuss the overall uncertainty of M_{BC} measurement in detail.

3. Measurements of b_{abs} by COSMOS and PSAP in the Arctic

COSMOS measures b_{abs} of BC particles deposited on quartz filters (Pallflex, E70-2075W) at a wavelength (λ) of 565 nm. In Asia, the uncertainty of b_{abs} (COSMOS) has been found to be better than 10% for an integration time of 1 h [*Kondo et al.*, 2011b]. COSMOS was operated at Barrow from August 2012 to December 2015 and at Ny-Ålesund from April 2012 to December 2015 (Figure 1). The measurements of b_{abs} by COSMOS (b_{abs} (COSMOS)) and the derived M_{BC} (COSMOS) values were made by using a PM_1 impactor inlet (i.e., with a size cutoff at an aerodynamic diameter D_p of about 1 μm). COSMOS aspirates ambient air at a flow rate of 0.7 L min^{-1} at standard temperature and pressure (STP: 273.15 K, 1013 hPa). The time resolution of the measurement was maintained at 1 min.

Kondo et al. [2011b] and *Miyakawa et al.* [2016] showed that the accuracy of M_{BC} (COSMOS) measurements is approximately 10% through extensive comparisons with M_{BC} measurements made by SP2 and EC measurements made by the TOT technique at several sites in Asia. They demonstrated that SP2, TOT (EC), and COSMOS measurements are consistent in the Asian region. By this comparison, MAC was determined to be about 10.0 m^2 g^{-1} by using $B = 1.22$ in equation (3). In the present study, we used $B = 1.397$ for the comparison of b_{abs} (COSMOS) with b_{abs} (PSAP). With a B value of 1.397, MAC (COSMOS) must be $10.0 \times (1.22/1.397) = 8.73$ m^2 g^{-1}. Different (B, MAC) combinations, for example, (1.22, 10.0 m^2 g^{-1}) and (1.397, 8.73 m^2 g^{-1}), result in an identical M_{BC} (COSMOS) value.

The M_{BC} (COSMOS)/M_{BC} (SP2) ratio was observed to decrease by about 7% with an increase in the mass median diameter (MMD) of 50 nm (from 130 to 180 nm) in Tokyo, possibly owing to the size dependence between MAC (COSMOS) and f_{fil} [*Kondo et al.*, 2011b; *Kondo*, 2015]. In Tokyo, the mean MMD was 146 ± 12 nm, with a mean geometrical standard deviation (σ_{gm}) of 1.82 ± 0.14. Considering the variability of the observed size distribution in Asia and the Arctic (MMD mostly up to about 200 nm) [*Kondo*, 2015], we estimated the typical uncertainty in M_{BC} (COSMOS) in the Arctic associated with the variability in BC size distribution to be about 10%. M_{BC} (PSAP) should also be influenced by this effect, although the degree of influence may be different owing to internal mixing of BC particles.

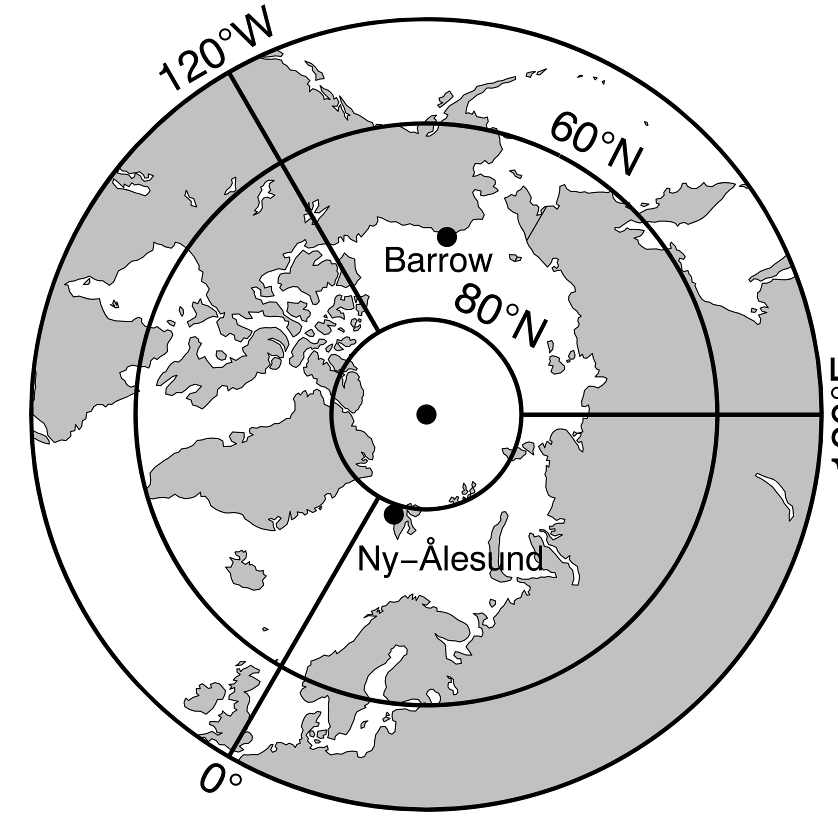

Figure 1. Map of the Arctic showing the locations of Barrow, Alaska, and Ny-Ålesund, Spitsbergen, where the BC measurements were made.

In this study, we also used b_{abs} data obtained with a PSAP and a continuous light absorption photometer (CLAP) [*Lack et al.*, 2014]. The CLAP is conceptually similar to PSAP but uses a solenoid valve to cycle through eight sample filter spots. Brief descriptions of the PSAP and CLAP measurements at Barrow and Ny-Ålesund are given here, and more details are provided in section A1. At these sites, all three instruments (PSAP, CLAP, and COSMOS) collected aerosol particles containing BC on the same type of fiber filter (Pallflex, type E70-2075W). The PSAP and CLAP measured b_{abs} of aerosol particles collected on the filter at $\lambda = 529$ nm and 522 nm, respectively, and both the PSAP and CLAP aspirated ambient air at a volumetric flow rate of 1 L min^{-1} (about 0.9 L min^{-1} at STP) using PM_1 and PM_{10} ($D_p < 10$ μm) impactors alternately for 30 min of each hour. The values of b_{abs} measured by PSAP (b_{abs} (PSAP)) and CLAP (b_{abs} (CLAP)) at different wavelengths were adjusted to 550 nm, to match the wavelength used for measurement of the scattering coefficient (b_{sca}) by nephelometer (Model 3563, TSI Inc.). We used a conversion coefficient of about 0.96 ± 0.01, assuming a dependence of b_{abs} (PSAP) of λ^{-1} or $\lambda^{-0.5}$ [*Ogren*, 2010]. Similarly, the coefficient of conversion from $\lambda = 550$ nm for PSAP to $\lambda = 565$ nm for COSMOS was 0.980 ± 0.007.

The uncertainty of the 1 h average b_{abs} (PSAP) was estimated to be about 20% at midlatitudes (35°N–45°N), considering instrumental noise and calibration following *Bond et al.* [1999], and unit-to-unit variability [*Sherman et al.*, 2015]. In this study, we used CLAP data obtained at Barrow between August 2012 and December 2015. The daily mean b_{abs} (PSAP) and b_{abs} (CLAP) values agreed to within 2% during 2012–2015. Therefore, for simplicity, we consider the instruments to be equivalent and refer to CLAP data as PSAP data hereafter.

Similarly, at Ny-Ålesund, measurements of b_{abs} at 532 nm were also carried out at about 10 m above the ground by using a custom-built PSAP [*Krecl et al.*, 2007]. No cyclone or impactor was used, so there was no particle size cutoff for the PSAP data obtained at Ny-Ålesund. However, it is unlikely that a substantial number of particles with $D_p > 10$ μm were included in the PSAP measurements, given the particle losses in the inlet system. Therefore, for simplicity, we refer to these data as PM_{10} data for comparison with the Barrow data. This simplification did not have a significant effect on the results of the present analysis.

The Arctic has basically two seasons. Therefore, for the analyses, the M_{BC} (COSMOS) and M_{BC} (PSAP) data were classified into winter (November–April) and summer (May–October) seasons.

4. Effect of Sea-Salt Particles on M_{BC} Measured by COSMOS

4.1. Laboratory Experiments

As discussed in section 3, in COSMOS measurements, light transmittance through a filter matrix is reduced by light scattering by refractory aerosol particles such as sea salt (predominantly NaCl) and mineral dust. Sea-salt particles are reported to constitute about 20% of the mass concentration of aerosols with diameters less than 1 μm at Barrow [*Quinn et al.*, 2002].

To assess the interference from sea-salt particles on M_{BC} (COSMOS), we performed laboratory experiments, as shown schematically in Figure 2. The aim of the experiments was to estimate the decrease in transmittance per unit scattering coefficient or volume (mass) of sea-salt particles. The refractive indices of NaCl are 1.54 and 1.55 at $\lambda = 589$ nm and 565 nm, respectively, whereas the refractive indices of polystyrene latex (PSL) are 1.59 and 1.60 at $\lambda = 589$ nm and 486 nm, respectively. Given that NaCl constitutes the major fraction of sea-salt particles [*Barrie and Barrie*, 1990], it is likely that sea-salt particles and PSL have similar optical effects on M_{BC} (COSMOS). Thus, in our experiments, we used PSL, which does not evaporate at 300°C, as a surrogate for sea-salt particles, which are not accurately sized by our calibration system because they are not spherical.

Water samples containing PSL particles were introduced by a peristaltic pump into a nebulizer at a constant flow rate (Figure 2a). The nebulizer then aerosolized PSL particles from the water suspension and passed them to a differential mobility analyzer (Model 3081, TSI Inc., MN, USA) for size segregation according to their mobility diameters. Monomodal PSL particles with diameters of 254 nm, 506 nm, and 814 nm were then sampled by COSMOS and SP2. The light-scattering data from the SP2 were used to derive the number concentration of PSL particles from the light-scattering data.

The scattering coefficient (Mm^{-1}) of the PSL particles at $\lambda = 565$ nm (b_{sca} (PSL)) was calculated from their number concentration as measured by the SP2 on the basis of Mie theory. The volume concentration (V_{PSL}, $\mu m^3\ cm^{-3}$) of the extracted PSL particles was also calculated from their number concentration and known diameter. The measured transmittance change of COSMOS due to PSL particles deposited on the filter was converted to the apparent BC mass concentration, denoted as ΔM_{BC} ($\mu g\ m^{-3}$).

ΔM_{BC} correlated well with b_{sca} (PSL) (Figure 3). As expected, ΔM_{BC} also correlated well with V_{PSL} (not shown). The $\Delta M_{BC}/b_{sca}$ (PSL) ratios, which showed only small dependence on the PSL diameters, were found to be about 0.0021 $\mu g\ m^{-3}/Mm^{-1}$. The $\Delta M_{BC}/V_{PSL}$ ratios, which also showed little dependence on the PSL diameters, were found to be about 0.022 $\mu g\ m^{-3}/10^{-6}\ cm^3\ m^{-3}$. The observed size dependence on PSL diameter was significantly smaller than that calculated on the basis of Mie theory for airborne PSL particles [*Moteki et al.*, 2010].

Considering these results, we used an average $\Delta M_{BC}/b_{sca}$ (PSL) ratio of 0.0021 $\mu g\ m^{-3}/Mm^{-1}$ for the subsequent analysis as follows:

$$\Delta M_{BC}\left(\mu g\ m^{-3}\right) = 0.0021\left[\mu g\ m^{-3}/Mm^{-1}\right] \times b_{sca}(PSL)\left[Mm^{-1}\right]. \quad (6)$$

Using this relationship, we also estimated f_{sca} in equation (2) as $f_{sca} = 0.0021$ ($g\ m^{-3}/m^{-1}$) × MAC (COSMOS) ($m^2\ g^{-1}$) = 0.0021 × 8.73 = 0.018. This value is very similar to the value of 0.016 derived by *Bond et al.* [1999] by using polydisperse LSPs ($(NH_4)_2SO_4$ and NaCl) (section 2). This agreement indicates that equation (6) is consistent with their measurement of the effect of LSPs on b_{abs} (PSAP).

To further ascertain whether the relationship represented by equation (6) is valid for ambient M_{BC} measurements, we conducted an additional experiment with a different configuration (Figure 2b). In the second experiment, ambient air containing BC particles was mixed with air containing PSL particles with a diameter of 506 nm and subsequently heated to 300°C. An SP2 was used to measure the BC mass concentration and the PSL number concentration, and then we derived the scattering coefficient of PSL from these measurements.

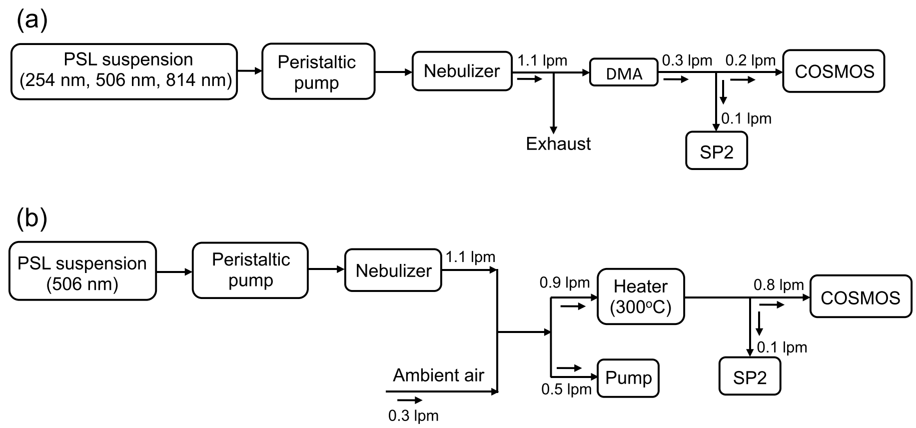

Figure 2. Experimental setup for the estimation of the decrease in transmittance per unit scattering coefficient or volume (mass) concentration of sea-salt particles in COSMOS M_{BC} measurements. (a) Water samples containing polystyrene latex (PSL) particles are introduced by a peristaltic pump into a nebulizer at a constant flow rate of 3.0×10^{-6} L s^{-1}. The nebulizer aerosolizes the PSL particles from a water suspension in dry air at a constant flow rate of 16 cm^3 s^{-1} at STP (273.15 K, 1013 hPa) and then passes the aerosol to a differential mobility analyzer (DMA) for mobility size segregation. Monomodal PSL particles with sizes of 254 nm, 506 nm, and 814 nm are sampled by COSMOS and a single particle soot photometer (SP2). (b) Same as Figure 2a but PSL particles with a diameter of 506 nm are mixed with ambient air containing BC particles and the mixture is heated at 300°C before being sampled by COSMOS and SP2.

$\Delta M_{BC}/b_{sca}$ (PSL) was approximately 0.0025 µg m^{-3}/Mm^{-1} (correlations not shown). This value is similar to that obtained in the first experiment, indicating that interference from a mixture of BC and sea-salt particles is very similar to interference from sea-salt particles alone. We used equation (6) to estimate the error due to sea-salt aerosol particles, as described in section 4.2.

4.2. Error Estimation

For the measurements of the sea-salt mass concentration ($M_{s\text{-}s}$) at Barrow, ambient air samples were collected through an inlet mounted 10 m above the ground onto filters by using PM_1 and PM_{10} impactors at 1 to 4 day intervals between October 1997 and December 2009. At Ny-Ålesund, air samples containing sea-salt particles

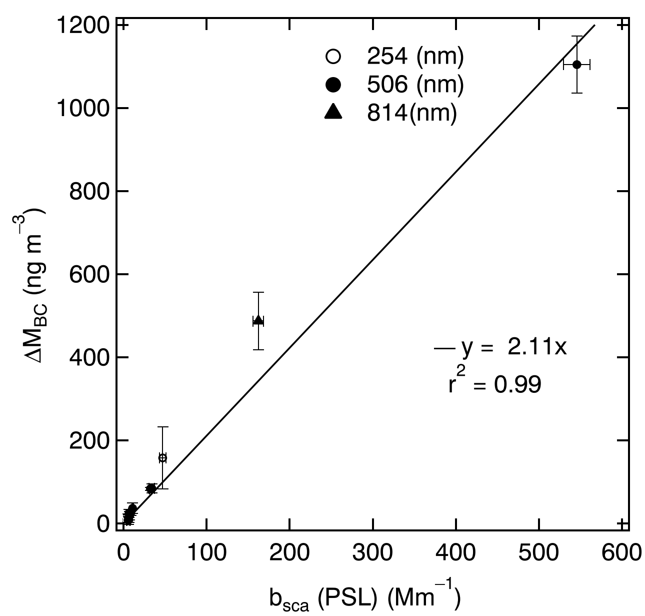

Figure 3. Relationship between the measured apparent BC mass concentration (ΔM_{BC}) and the scattering coefficient of PSL particles (b_{sca} (PSL)) with diameters of 254 nm, 506 nm, and 814 nm, calculated from number concentrations measured by SP2. Note that the regression line fit was forced through origin (intercept = 0).

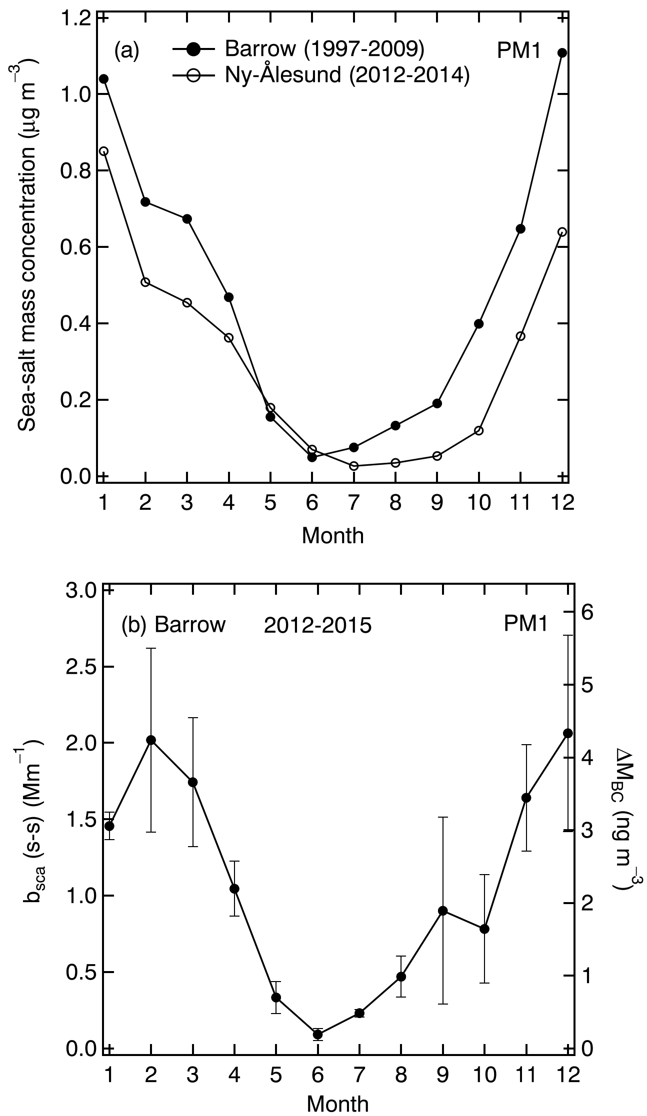

Figure 4. (a) Monthly mean mass concentrations of sea-salt particles at Barrow from October 1997 to December 2009 and at Ny-Ålesund from January 2012 to December 2014. (b) Monthly mean scattering coefficients of sea-salt particles (b_{sca} (*s-s*)) and corresponding apparent BC mass concentrations (ΔM_{BC}). The vertical bars represent the standard deviations ($\pm 1\sigma$) of the monthly mean values.

were collected daily from January 2012 to December 2014 without use of an impactor. For simplicity, we also designated these data as PM_{10}. More detailed descriptions of the $M_{s\text{-}s}$ measurements are presented in section A2.

$M_{s\text{-}s}$ was calculated from measured Na^+ and Cl^- with equation (7) [*Holland*, 1978].

$$M_{s\text{-}s}\left(\mu g\ m^{-3}\right) = Cl\left(\mu g\ m^{-3}\right) + Na\left(\mu g\ m^{-3}\right) \times 1.47. \quad (7)$$

The factor 1.47 is the $(Na + K + Mg + Ca + SO_4 + HCO_3)/Na$ seawater ratio. The uncertainty arising from the use of equation (7) to estimate $M_{s\text{-}s}$ is described in section A2.

At both sites, $M_{s\text{-}s}$ showed similar and notable seasonal variations; values were about an order of magnitude higher in winter (about 1 $\mu g\ m^{-3}$) than in summer (about 0.1 $\mu g\ m^{-3}$) (Figure 4a). The seasonality and magnitude of $M_{s\text{-}s}$ at Barrow during 1997–2009 were very similar to those from October 1997 to December 2000 [*Quinn et al.*, 2002]. This similarity suggests that the interannual variability of $M_{s\text{-}s}$ is relatively small.

To estimate ΔM_{BC} we first calculated the contribution of sea-salt aerosols to b_{sca} for PM_1 aerosols (b_{sca} (PM_1)) measured at Barrow. For this calculation, we used mass concentrations and the scattering coefficient for PM_1 aerosols measured at Barrow between 1997 and 2000 [*Quinn et al.*, 2002]. The scattering coefficient of sea salt (b_{sca} (*s-s*)) and b_{sca} (PM_1) can be calculated with equations (8a) and (8b). The monthly averaged values of these parameters, (b_{sca} (s-s))$_{av}$ and (b_{sca} (PM_1))$_{av}$, were obtained from *Quinn et al.* [2002, Tables 2 and 4].

$$[b_{sca}(s\text{-}s)]_{av} = \alpha_{s\text{-}s} \times [M_{s\text{-}s}]_{av}, \tag{8a}$$

$$[b_{sca}(PM_1)]_{av} = \alpha_{PM1} \times [M_{PM1}]_{av}, \tag{8b}$$

where $[M_{s\text{-}s}]_{av}$ and $[M_{PM1}]_{av}$ are monthly averaged mass concentrations of sea-salt and PM_1 aerosols, respectively, and $\alpha_{s\text{-}s}$ and α_{PM1} are the mass-scattering efficiencies ($m^2\,g^{-1}$) of sea-salt and total aerosols, respectively, for PM_1.

The $[f_{s\text{-}s}]_{av} = [b_{sca}\ (s\text{-}s)]_{av}/[b_{sca}\ (PM_1)]_{av}$ ratio ranged between 0.06 and 0.38 with an annual average of 0.24. We used monthly averaged b_{sca} (PM_1) observed from August 2012 to December 2015 to estimate the monthly averaged b_{sca} (*s-s*) by the following equation:

$$b_{sca}(s\text{-}s) = [f_{s\text{-}s}]_{av} \times b_{sca}(PM_1). \tag{9}$$

Finally, we calculated monthly mean ΔM_{BC} by replacing b_{sca} (PSL) in equation (6) with b_{sca} (*s-s*) (Figure 4b). At Barrow, ΔM_{BC} varied from about 0.19 to 4.3 ng m^{-3}, with a mean value of about 2.2 ng m^{-3}, which corresponds to about 9% of the annual mean M_{BC} (COSMOS).

Data similar to those used to derive ΔM_{BC} at Barrow were not available at Ny-Ålesund. However, ΔM_{BC} should be proportional to $M_{s\text{-}s}$, as shown by our laboratory experiments (section 4.1). At Ny-Ålesund, the $M_{s\text{-}s}$ values were about 30% lower than at Barrow (Figure 4a) and the yearly average ΔM_{BC} was estimated to be about 1.6 ng m^{-3}.

In addition to sea-salt particles, mineral dust particles may contribute to ΔM_{BC}, although reported mass concentrations of dust particles in the Arctic are much less than those of sea-salt particles [*Brock et al.*, 2011; *Quinn et al.*, 2002]. The variability in BC size distribution may cause an additional uncertainty. Therefore, comparisons of M_{BC} (COSMOS) with the measurements of M_{BC} by other reliable techniques, such as the comparisons we did in Asia, are critically important for evaluating the overall accuracy of M_{BC} (COSMOS) in the Arctic.

5. Comparisons of M_{BC} (COSMOS) With M_{EC} Measurements at Barrow and With M_{BC} (SP2) Measurements at Ny-Ålesund

5.1. Barrow

To evaluate the overall accuracy of M_{BC} (COSMOS), we carried out a detailed intercomparison between M_{BC} (COSMOS) and the mass concentration of EC measured by the TOT technique at Barrow. For each M_{EC} measurement, air samples were collected at Barrow between August 2012 and June 2013 on a quartz fiber filter (Tissuquartz Filters 2500 QAT-UP; 20 × 25 cm Pall Corporation) by using a Tisch high-volume sampler (TE-6070; Tisch Environmental Cleves, Ohio, USA) with a PM_{10} cutoff and a flow rate of about 1.2 m^3 min^{-1} at 10 m above ground level. The particle-laden filters were analyzed with a TOT carbon analyzer (Sunset Laboratories, Tigard, OR, USA), and M_{EC} was quantified following the temperature protocol recommended by the National Institute for Occupational Safety and Health (NIOSH 5040) [*Birch and Cary*, 1996]. The M_{EC} values are given in units of ng m^{-3} STP. We estimated the uncertainty of M_{EC} associated with the uncertainty of the flow rate of the filter sampling to be about 10%. We estimated the overall uncertainty of the M_{EC} measurement to be about 17% (excluding the uncertainty of the flow rate). More details of the EC measurements are given in section A3.

In Tokyo, the contributions of BC particles with diameters (D_{BC}) larger than 1 μm to M_{BC} of particles with diameters less than about 4 μm (PM_4) were observed to be less than 10%, based on SP2 measurements. At the remote site of Hedo (26.9°N, 128.3°E) on Okinawa Island, Japan, the contribution was about 8% in spring 2016

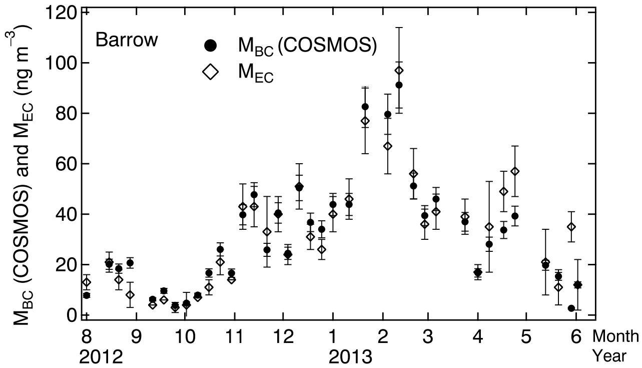

Figure 5. Time series of M_{BC} (COSMOS) and M_{EC} at Barrow between August 2012 and June 2013. The M_{BC} (COSMOS) data were averaged over the same period as the individual M_{EC} measurements.

(section A4, Figure A1a). BC particles become more active as cloud condensation nuclei as their diameters increase, and larger BC particles have been observed to be removed more efficiently by wet deposition than BC particles with smaller diameters [*Ohata et al.*, 2016; *Moteki et al.*, 2012; *Kondo et al.*, 2016]. BC particles larger than 1 μm should be scavenged more efficiently during long-range transport to the Arctic from lower latitudes. Therefore, it is unlikely that the contribution of BC particles larger than 1 μm to M_{BC} (i.e., PM_{10} minus PM_1) exceeds about 10% at Barrow; thus, the uncertainty in the comparison between M_{BC} (COSMOS) (PM_1) and M_{EC} (PM_{10}) should be similar at Barrow.

We averaged the 1 min M_{BC} (COSMOS) data over the same periods as the individual M_{EC} observations and compared the M_{EC} and M_{BC} (COSMOS) time series (Figure 5). The two measurements agreed very well throughout the year, and the monthly mean of the difference between M_{BC} (COSMOS) and M_{EC} did not show any clear seasonal variation (section A5, Figure A2). In most months, M_{BC} (COSMOS)-M_{EC} was less than 5 ng m^{-3}; this result is consistent with ΔM_{BC} estimated in section 4.2. Overall, this comparison indicates that the effect of sea-salt or mineral dust particles on M_{BC} (COSMOS) was less than 5 ng m^{-3}.

Moreover, M_{EC} and M_{BC} (COSMOS) were highly correlated ($r^2 = 0.92$) and the slope of the M_{EC}-M_{BC} (COSMOS) correlation was 0.99 (Figure 6). Because the COSMOS measurement is based on light absorption, the good

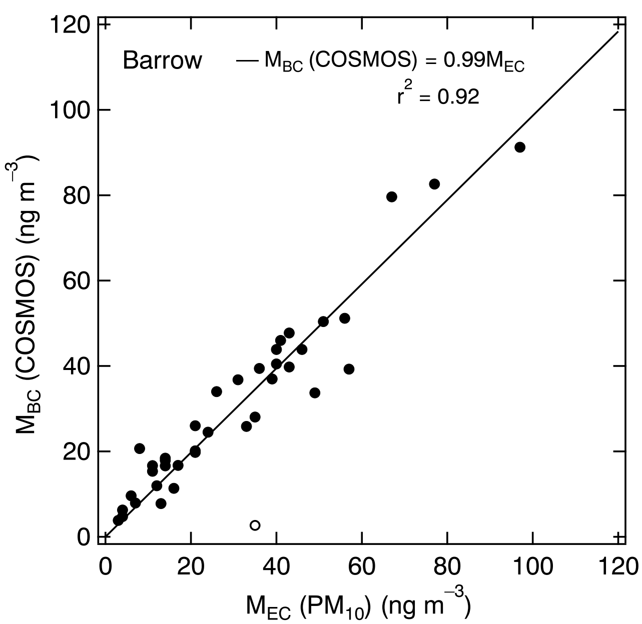

Figure 6. Correlation between M_{EC} and M_{BC} (COSMOS) at Barrow during August 2012 and June 2013. One outlier, shown as an open circle, was excluded from the least squares fitting.

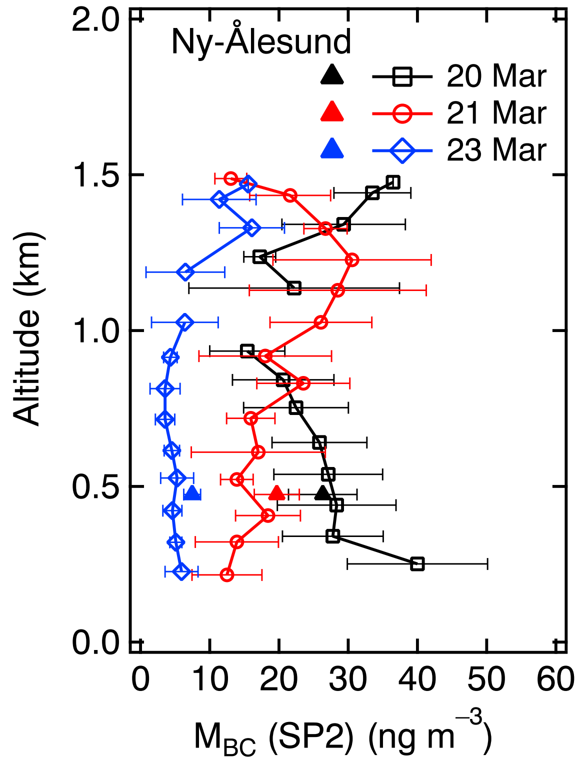

Figure 7. Vertical profiles of M_{BC} (SP2) measured on 20, 21, and 23 March 2013 during the ACCACIA campaign of aircraft observations. The vertical M_{BC} (SP2) profiles were obtained at locations within ±0.5° latitude and ±3° longitude from the Zeppelin station at Ny-Ålesund. M_{BC} (SP2) values from every 100 m altitude interval were binned, and the horizontal bars show the spatial variation (±1σ) in each bin. Daily mean M_{BC} (COSMOS) values at Ny-Ålesund on the days corresponding to the aircraft observations are shown by triangles.

agreement between M_{BC} (COSMOS) and M_{EC} indicates that BC is the dominant light-absorbing component of aerosols with diameters smaller than 1 µm at Barrow. It should be noted here that in Asia, MAC (COSMOS) was determined to be 8.73 $m^2 g^{-1}$ (or 10.0 $m^2 g^{-1}$ for $B = 1.22$) by comparing M_{BC} (COSMOS) with M_{BC} (SP2) and M_{EC} [*Kondo et al.*, 2011b]. The present results indicate that the same MAC (COSMOS) value can be applied to the BC measurements in the Arctic and they demonstrate the consistency and lack of regional dependence of MAC (COSMOS).

5.2. Ny-Ålesund

We compared M_{BC} (COSMOS) at Ny-Ålesund with aircraft M_{BC} (SP2) measurements conducted near Zeppelin station, Ny-Ålesund, for 3 days in March 2013, during the Aerosol-Cloud Coupling and Climate Interactions in the Arctic (ACCACIA) campaign [*Liu et al.*, 2015]. Detailed descriptions of the aircraft M_{BC} (SP2) measurements and calibration procedures are provided elsewhere [*Liu et al.*, 2015; *McMeeking et al.*, 2010]. In brief, BC size distributions were measured in the diameter range $D_{BC} = 69–478$ nm and M_{BC} (SP2) was obtained by integrating the BC mass size distributions with an accuracy of about 10% [*Liu et al.*, 2010].

We estimated BC mass concentrations between 478 nm and 1000 nm by fitting a lognormal function to the SP2 data (section A4, Figure A1b) and found that the mean contribution of BC mass concentrations between 478 nm and 1000 nm to M_{BC} (SP2) for PM_1 was about 15%. In the comparison with M_{BC} (COSMOS), we corrected the M_{BC} (SP2) data for this additional contribution.

Daily mean M_{BC} (COSMOS) at Ny-Ålesund agreed well to within about 3% ($r^2 = 0.96$) with the vertical profiles of M_{BC} (SP2), in units of ng m^{-3} STP, obtained on 20, 21, and 23 March 2013 with an uncertainty of 15% (Figure 7 and section A6). The absolute difference between M_{BC} (COSMOS) and M_{BC} (SP2) was less than 4 ng m^{-3}, despite the temporal and spatial differences of these data (Figure A3).

6. COSMOS and PSAP Intercomparison at Barrow and Ny-Ålesund

Although in this paper we do not present a detailed interpretation of the variability in b_{sca}, it is useful to examine temporal variations of b_{sca}, which is used in equation (2) to derive b_{abs} (PSAP) at Barrow and Ny-Ålesund. At Barrow, daily b_{sca} values varied between about 1 and 20 Mm^{-1}, with an annual mean of 4.1 ± 3.5 Mm^{-1} (Figure 8a); wintertime b_{abs}/b_{sca} ratios were higher by a factor of about 1.5 than the summertime ratios, and, as a result, the wintertime single scattering albedo, defined as SSA = b_{sca}/(b_{abs} (PSAP) + b_{sca}), of 0.94 ± 0.03, was lower than the summertime value (0.96 ± 0.04) (section A7). At Ny-Ålesund, daily b_{sca} values ranged between about 0.1 and 18 Mm^{-1}, with an annual mean of 4.0 ± 3.5 Mm^{-1} (Figure 8b), and wintertime b_{abs}/b_{sca} ratios were higher by a factor of about 1.3 than the summertime ratios. The corresponding SSA values were 0.95 ± 0.05 and 0.96 ± 0.04 in winter and summer, respectively (section A7). These results suggest that the contribution of absorbing particles to the total aerosol extinction coefficient was larger during winter at both sites.

We also compared b_{abs} (COSMOS) and b_{abs} (PSAP) at Barrow and Ny-Ålesund. At Barrow, about 36% of the daily b_{abs} (PSAP) values were less than 0.1 Mm^{-1} and b_{abs} (PSAP) rarely exceeded 1 Mm^{-1} (Figure 8a), whereas at Ny-Ålesund, about 60% of b_{abs} values were less than 0.1 Mm^{-1} and higher values ($b_{abs} > 1$ Mm^{-1}) were seldom observed (Figure 8b).

b_{abs} (PSAP) (PM_1) was highly correlated with b_{abs} (PSAP) (PM_{10}) ($r^2 = 0.97$) at Barrow (Figure 9a). The slope of the correlation, denoted as β, was 0.85. Even when the symmetrical least squares fit was computed, β was little changed owing to the relatively high correlation between the parameters ($r^2 > 0.82$).

Light-absorbing particles with diameters larger than 1 μm, including mineral dust particles and BC, likely contribute to b_{abs} (PSAP) for PM_{10}. In addition, correction of the scattering effects may be size-dependent, which is not fully taken into account by the correction made with equation (2). As discussed in section 5.1, it is unlikely that the BC mass concentration fraction with particle diameters larger than 1 μm exceeds 10%. Moreover, the MAC for BC particles larger than 1 μm is considerably smaller than that for BC particles smaller than 1 μm [*Schwarz et al.*, 2013]. Therefore, it is likely that the contribution of BC particles larger than 1 μm is limited. It is difficult to identify the reason for the slope being less than 1, owing to the lack of sufficient data necessary to quantify these effects.

b_{abs} (COSMOS) was highly correlated with both b_{abs} (PSAP) for PM_1 ($r^2 = 0.87$; $\beta = 0.82$) and PM_{10} ($r^2 = 0.88$; $\beta = 0.72$) at Barrow, although some data points deviated significantly from the least squares fitted line (Figures 9b and 9c). The β value of 0.72 is largely explained by the product of the slopes = 0.85 (PSAP (PM_{10}) − PSAP (PM_1)) × 0.82 (COSMOS − PSAP (PM_1)) = 0.70.

It is possible that the b_{abs} (PSAP)-b_{abs} (COSMOS) correlation with β less than 1 and the occasional large scatter between b_{abs} (PSAP) and b_{abs} (COSMOS) for PM_1 at Barrow are partly due to differences in the methodology used to derive b_{abs}: equation (2) for PSAP data, whereas equation (4) for COSMOS data. The subtraction of the effect of scattering by non-BC aerosols in equation (2) may add uncertainty to the absolute accuracy and precision of b_{abs} (PSAP). In addition, light absorption of internally mixed BC particles collected on filters is enhanced by the lens effect in a PSAP, whereas this effect is negligibly small for COSMOS, as discussed in section 2. Further, there may exist volatile light-absorbing aerosol species that affect b_{abs} (PSAP) but not b_{abs} (COSMOS). The combined effect of these factors is that nonabsorbing coatings or non-BC absorbers may contribute to an enhancement of up to 22% (1/0.82) of the absorption of uncoated BC particles. It should be noted that differences in the absolute value of b_{abs} do not influence the M_{BC} values derived from PSAP data, as discussed below.

At Ny-Ålesund, b_{abs} (COSMOS) and b_{abs} (PSAP) for PM_{10} were also correlated ($r^2 = 0.82$; $\beta = 0.70$) (Figure 9d). b_{abs} (PSAP) was higher than b_{abs} (COSMOS) by 43% (1/0.70) at Ny-Ålesund (PM_{10}). The slope (0.70) agrees with that obtained at Barrow to within 3%. Because β for PM_{10} was similar between the two sites, we used b_{abs} (PSAP) for PM_{10} to derive M_{BC} at Ny-Ålesund.

Finally, it is possible to derive the mass concentration of BC by using the b_{abs} (PSAP) data and applying these empirically determined relationships. Equation (10) is the condition of scaling of M_{BC} (PSAP) by M_{BC} (COSMOS):

$$M_{BC}(\text{PSAP}) = M_{BC}(\text{COSMOS}). \tag{10}$$

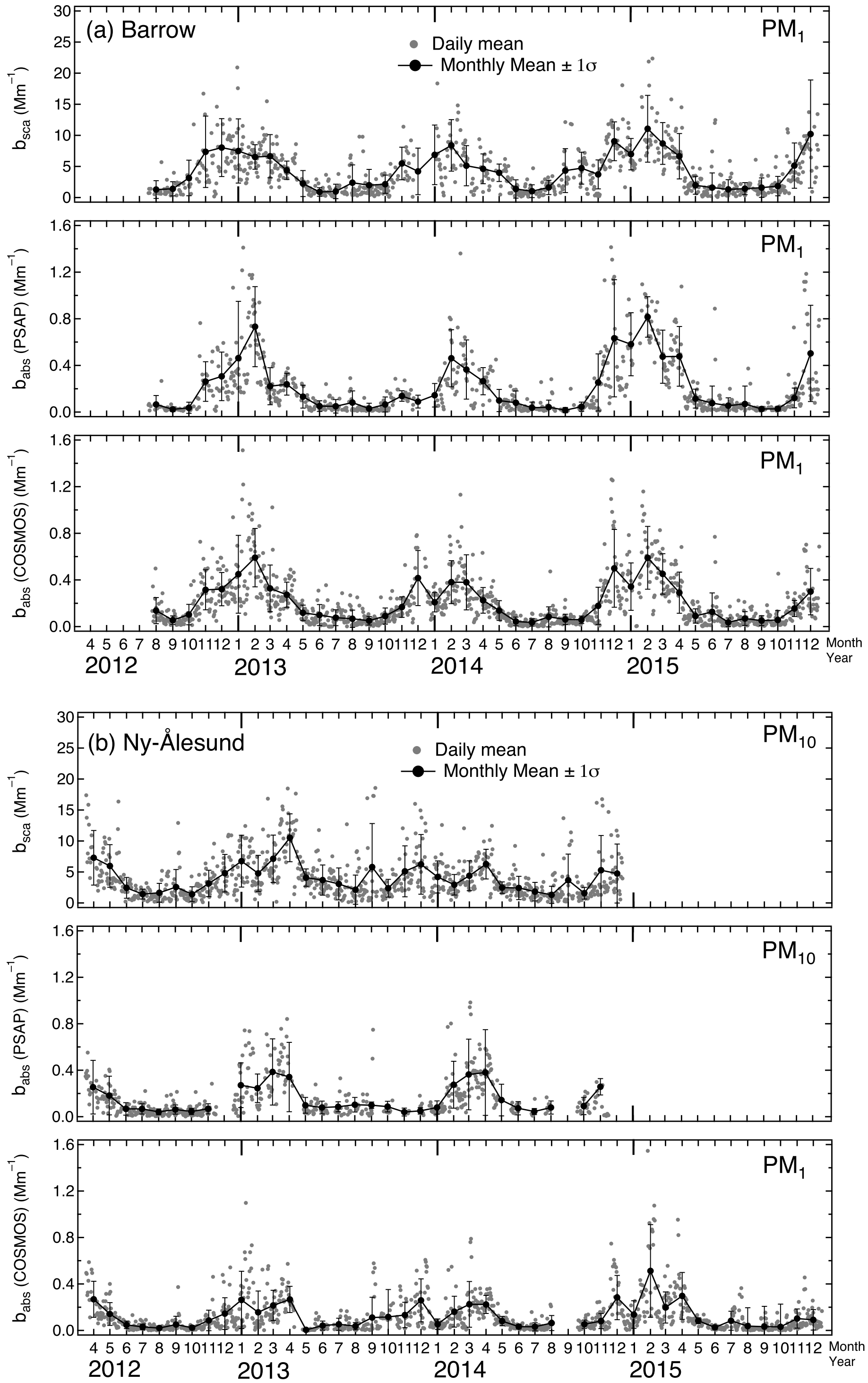

Figure 8. (a) Daily and monthly mean values of b_{sca} (measured by nephelometer), b_{abs} (PSAP), and b_{abs} (COSMOS) for PM_1 at Barrow from 2012 to 2015. (b) Same as Figure 8a but at Ny-Ålesund for PM_{10} during 2012–2014. The gaps in the PSAP and COSMOS data at Ny-Ålesund are due to the data quality assurance procedure.

At Barrow,

$$M_{BC}(\text{PSAP}) = \beta \times b_{abs}(\text{PSAP})/\text{MAC (COSMOS)}, \quad (11)$$

where $\beta = 0.82 \pm 0.01$ ($\pm 1\sigma$), and MAC (COSMOS) = 8.73 m^2 g^{-1}.

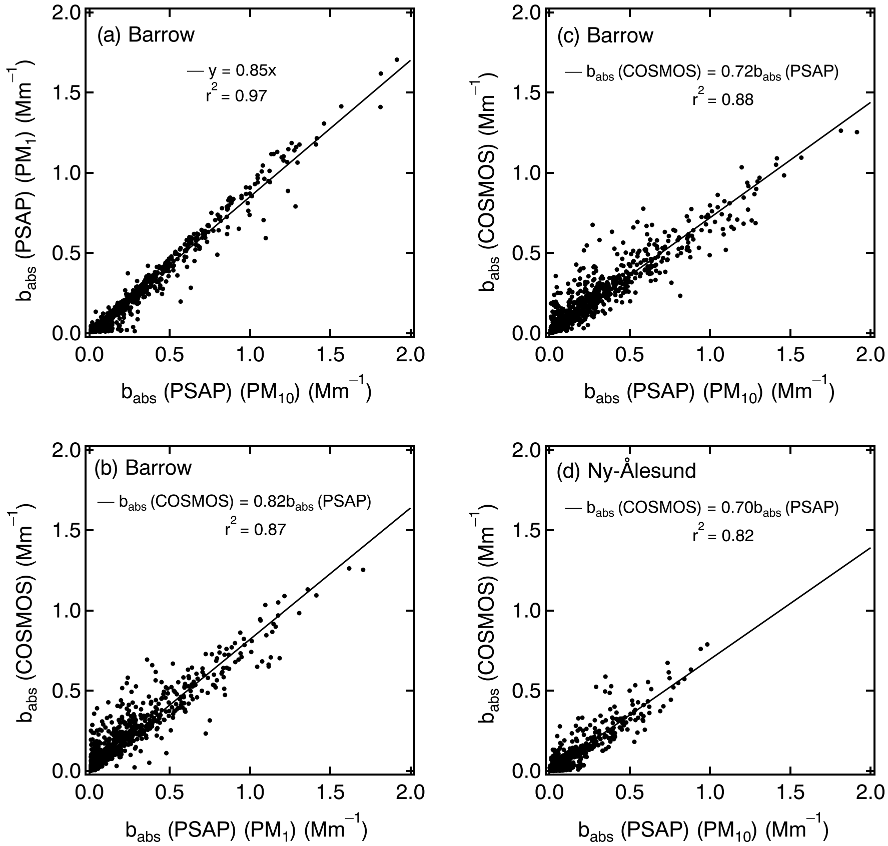

Figure 9. Scatterplots between daily mean (a) b_{abs} (PSAP) for PM_1 and b_{abs} (PSAP) for PM_{10} and between daily mean b_{abs} (COSMOS) and b_{abs} (PSAP) for (b) PM_1 and (c) PM_{10} at Barrow during 2012–2015. (d) Scatterplot between daily mean b_{abs} (COSMOS) and b_{abs} (PSAP) for PM_{10} at Ny-Ålesund during 2012–2014.

MAC (PSAP) is expressed as follows:

$$\text{MAC (PSAP)} = \text{MAC (COSMOS)}/\beta, \tag{12}$$

where MAC (PSAP) = $10.6 \pm 0.2\ m^2\ g^{-1}$ for PM_1. At Ny-Ålesund, $\beta = 0.70 \pm 0.01$ and MAC (PSAP) = $12.5 \pm 0.2\ m^2\ g^{-1}$ for PM_{10}.

MAC (PSAP) values were also derived for each year by using the corresponding comparison between COSMOS and PSAP measurements at Barrow and Ny-Ålesund. The derived MAC (PSAP) values varied between 8.5 and 11.8 $m^2\ g^{-1}$ (PM_1) during 2012–2015 at Barrow and between 9.5 and 13.4 $m^2\ g^{-1}$ (PM_{10})

Table 2. Slopes and Correlation Coefficients of the Relationship Between b_{abs} (COSMOS) and b_{abs} (PSAP) at Barrow (August 2012 to December 2015) and Ny-Ålesund (April 2012 to December 2014) in Individual Years and the Corresponding MAC (PSAP) Values[a]

	Barrow			Ny-Ålesund		
ear	Slope ± 1σ	r^2	MAC (PSAP) ($m^2\ g^{-1}$)	Slope ± 1σ	r^2	MAC (PSAP) ($m^2\ g^{-1}$)
2012	1.07 ± 0.049	0.76	8.5	0.92 ± 0.031	0.72	9.5
2013	0.92 ± 0.016	0.89	9.5	0.65 ± 0.016	0.82	13.4
2014	0.82 ± 0.014	0.91	10.7	0.65 ± 0.010	0.92	13.4
2015	0.74 ± 0.010	0.92	11.8			
Average 1			10.1 ± 1.4			12.1 ± 2.3
Average 2	0.82 ± 0.01	0.87	10.6 ± 0.2	0.72 ± 0.01	0.82	12.5 ± 0.2

[a]Average 1 was calculated by averaging the MAC (PSAP) values of the individual years. Average 2 are the regression results and the MAC (PSAP) value derived from the correlation of all b_{abs} (PSAP) and b_{abs} (COSMOS) values.

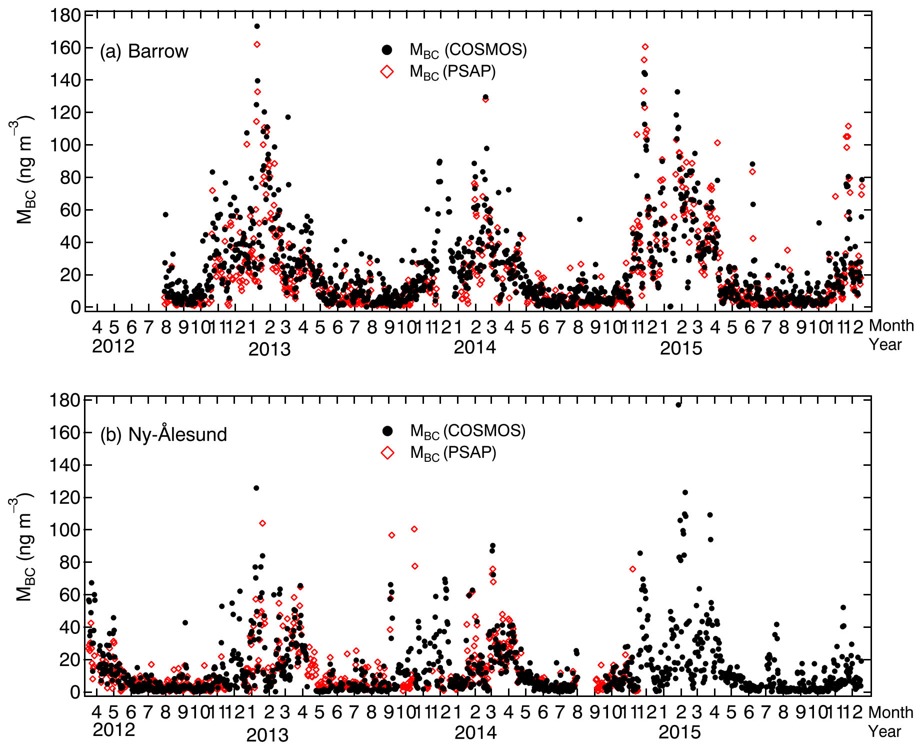

Figure 10. Time series of daily mean M_{BC} (COSMOS) and M_{BC} (PSAP) at (a) Barrow (2012–2015) and (b) Ny-Ålesund (2012–2015).

during 2012–2014 at Ny-Ålesund (Table 2). At Barrow, we estimated the MAC (PSAP) accuracy to be about 18%, taking into account the slope determination accuracy of about 2%, the M_{BC} (COSMOS) accuracy of 10%, and the year-to-year variability in MAC (PSAP) of about 15% (1σ). Similarly, at Ny-Ålesund, we estimated the accuracy of MAC (PSAP) to be about 20%, taking into account the year-to-year variability in MAC (PSAP) of about 18% (1σ).

We examined time series of daily mean M_{BC} (COSMOS) and M_{BC} (PSAP) for the entire period (2012–2015) of COSMOS measurements at both sites to evaluate the consistency of these two instruments (Figure 10). The temporal variations of M_{BC} (COSMOS) and those of M_{BC} (PSAP) were generally well correlated over wide ranges of values, as expected from the high correlation between b_{abs} (PSAP) and b_{abs} (COSMOS) (Figure 9) and the scaling of b_{abs} (PSAP) in equation (10). The time series qualitatively show the degree of the differences between individual daily mean values of M_{BC} (COSMOS) and M_{BC} (PSAP). The difference between monthly mean M_{BC} (COSMOS) and M_{BC} (PSAP) values was generally less than 10 ng m^{-3} (section A8.1, Figure A5) and agreed to within 5% ($r^2 = 0.96$) and 2% ($r^2 = 0.95$) at Barrow and Ny-Ålesund, respectively (section A8.2, Figure A6). It is not known whether the relationship between the PSAP and COSMOS measurements observed in the Arctic holds at other latitudes.

7. Temporal Variations of M_{BC}

7.1. Year-to-Year Variability

M_{BC} (COSMOS) did not show well-defined diurnal variations (monthly mean diurnal variation <10% of the daily mean) at these sites during any part of the year (section A9), suggesting that localized BC emissions from anthropogenic activities had little influence on the measured M_{BC}.

It is important to investigate year-to-year variations of M_{BC} in the Arctic with reliable data sets because year-to-year variations in BC emissions and transport pathways can be reflected in M_{BC} changes. As we showed in section 6, it is possible to use M_{BC} (PSAP) for this purpose. We examined time series of monthly mean M_{BC} (PSAP) from January 1998 to July 2012 at Barrow and from April 2006 to March 2012 at Ny-Ålesund.

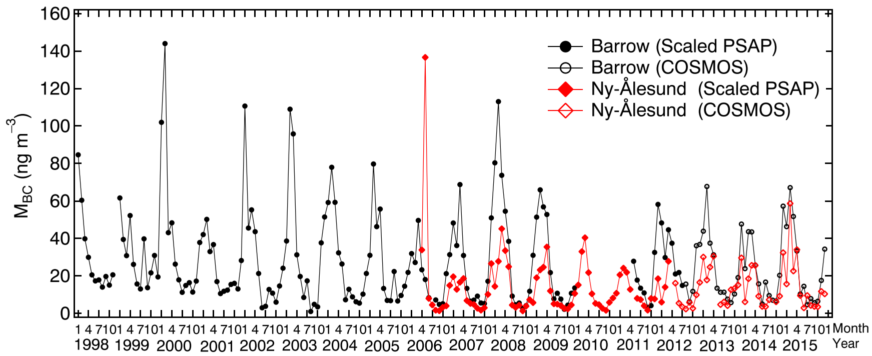

Figure 11. Time series of monthly mean M_{BC} (PSAP) values at Barrow (January 1998 to July 2012) (closed circles) and Ny-Ålesund (April 2006 to March 2012) (closed diamonds). The series are extended to December 2015 with M_{BC} (COSMOS) values at Barrow (open circles) and Ny-Ålesund (open diamonds). The gap in the PSAP data at Barrow from January 2010 to April 2011 was caused by an instrument malfunction.

Monthly mean M_{BC} (COSMOS) values at these sites also partly overlap these time series and extend them up to December 2015 (Figure 11). PSAP data are missing at Barrow from January 2010 to April 2011 because of an instrument malfunction.

In winter, M_{BC} showed year-to-year variations of up to a factor of two with a relative variability of about 22% (1σ). In summer, M_{BC} was much lower than it was in winter and year-to-year variability in M_{BC} was correspondingly lower; the relative variability in M_{BC} was about 36% (1σ) in summer. Year-to-year variability can be caused by variations in BC emissions, especially those due to biomass burning, as well as by differences in the transport pathway and the degree of the wet deposition of BC during transport.

Relatively high M_{BC} values were observed in winter 2008 at Barrow (Figure 11). During winter 2008, the BC profiles observed by the Aerosol, Radiation, and Cloud Processes affecting Arctic Climate aircraft observations indicated downward transport of BC from the free troposphere to the planetary boundary layer over the Alaskan Arctic [*Spackman et al.*, 2010; *Brock et al.*, 2011]; these findings suggest that biomass burning events in Siberia (Russia) and Kazakhstan influenced the surface-measured M_{BC} at Barrow in winter 2008. More detailed studies of the effects of the temporal variations of the emission and transport of BC on the surface M_{BC} in the Arctic require simulations with sophisticated numerical models, which are beyond the scope of this study.

7.2. Long-Term Trends

At Barrow, *Quinn et al.* [2007] showed that there was a significant decreasing trend in b_{abs} (PSAP) (PM_{10}) at 550 nm in the months of March and April between 1998 and 2006. Here we extended the period of the measurements to 1998–2015 and investigated the long-term changes of M_{BC} (PSAP) in winter and summer.

We applied the least squares (LS) method to time series of M_{BC} (PSAP) averaged over winter and summer seasons from 1998 to 2015 to obtain regression lines (Figure 12). The slopes derived by the LS method were -0.56 ± 0.45 ng m^{-3} yr^{-1} (-1.3% yr^{-1}) with $r^2 = 0.10$ for winter and -0.53 ± 0.17 ng m^{-3} yr^{-1} (-4.7% yr^{-1}) with $r^2 = 0.50$ for summer (Table 3).

It is noteworthy that after 2001, the changes in M_{BC} (PSAP) were small in summer (Figure 12). We therefore excluded the data for the initial 3 years and recalculated the slopes, obtaining values of -0.43 ± 0.56 ng m^{-3} yr^{-1} (-1.3% yr^{-1}) with $r^2 = 0.05$ for winter and -0.23 ± 0.13 ng m^{-3} yr^{-1} (-1.7% yr^{-1}) with $r^2 = 0.20$ for summer (Table 3). We also derived the M_{BC} (PSAP) trends for 3 month periods between 1998 and 2015, but r^2 values were not substantially improved (section A10).

We also estimated the trends by a regression analysis of M_{BC} (PSAP) at Barrow against time based on the Bayesian statistical method [e.g., *Hoff*, 2009] (section A10). The expected value of the slope and its uncertainty were evaluated as the mean and standard deviation, respectively, of ~2×10^5 sampling points over the slope-intercept space obtained by the Markov chain Monte Carlo (MCMC) method. The trends derived by the

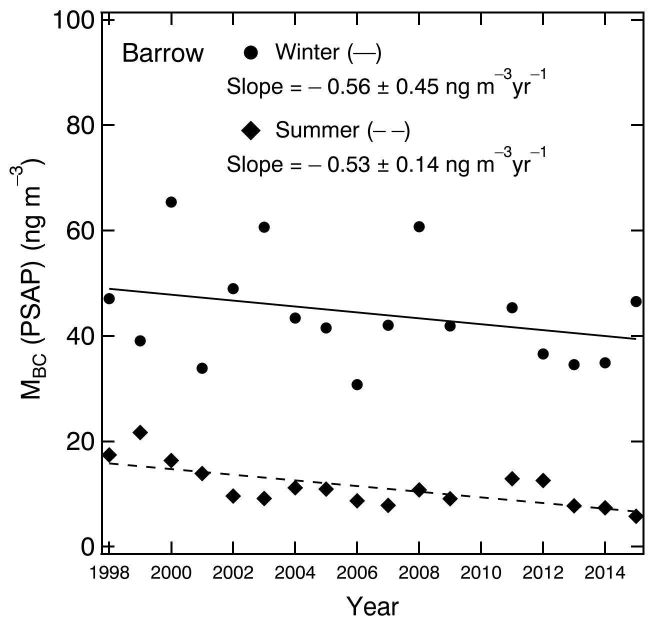

Figure 12. Time series of monthly mean M_{BC} (PSAP) in winter (November–April) and summer (May–October) during 1998–2015 at Barrow. The circles (winter) and diamonds (summer) represent seasonally averaged M_{BC} (PSAP) values. The regression lines were obtained by applying the least squares method to the M_{BC} (PSAP) time series.

MCMC method were statistically insignificant (not shown), although slopes were obtained for 3 month periods between 1998 and 2015 (Table A1). Both the LS and MCMC results indicate that it is difficult to derive the slopes of long-term M_{BC} (PSAP) changes accurately for the period 1998–2015. The lack of statistical reliability is due to the large year-to-year variability in M_{BC} (PSAP), which potentially includes the year-to-year variability of MAC (PSAP) (maximum about 20%; section A8.1).

Collaud Coen et al. [2013] derived b_{abs} (PSAP) (PM_{10}) trends at Barrow for the periods 1998–2010 and 2001–2010 by a different method and obtained slopes of $-1.3\%\ yr^{-1}$ (1998–2010) and $-6.5\%\ yr^{-1}$ (2001–2010). The much smaller slope for 1998–2009 than for 2001–2010 is qualitatively consistent with our analysis. However, they used different parameters. First, they used PM_{10} data, whereas we used PM_1 data, and second, they did not exclude the 2010 data, whereas we excluded anomalously low 2010 PM_1 values caused by a malfunction of the PSAP (section 7.1, Figure 11).

We could not perform a similar trend analysis of the Ny-Ålesund data owing to the lack of M_{BC} (PSAP) data with sufficient reliability prior to 2006.

7.3. Seasonal Variations

At Barrow, the monthly mean M_{BC} (COSMOS) averaged over the 3 year period from 2012 to 2015 agreed with the M_{BC} (PSAP) values averaged over the 10 year period from January 2005 to December 2015 to within 10% (Figure 13a), as expected from the trend analysis discussed in section 7.2. At Ny-Ålesund, monthly mean M_{BC}

Table 3. Trends of Seasonally Averaged M_{BC} (PSAP) Between 1998 and 2015 at Barrow[a]

Season	Slope ($ng\ m^{-3}\ yr^{-1}$) ± 1σ	r^2
Winter (November–April)	−0.56 ± 0.45	0.10
Summer (May–October)	−0.53 ± 0.14	0.50
Winter 2001–2015	−0.43 ± 0.56	0.05
Summer 2001–2015	−0.23 ± 0.13	0.20

[a]Linear trends estimated by least squares fitting are shown together with their ±1σ and r^2 values. The trends derived for M_{BC} (PSAP) in winter (2001–2015) and summer (2001–2015) are also shown for comparison.

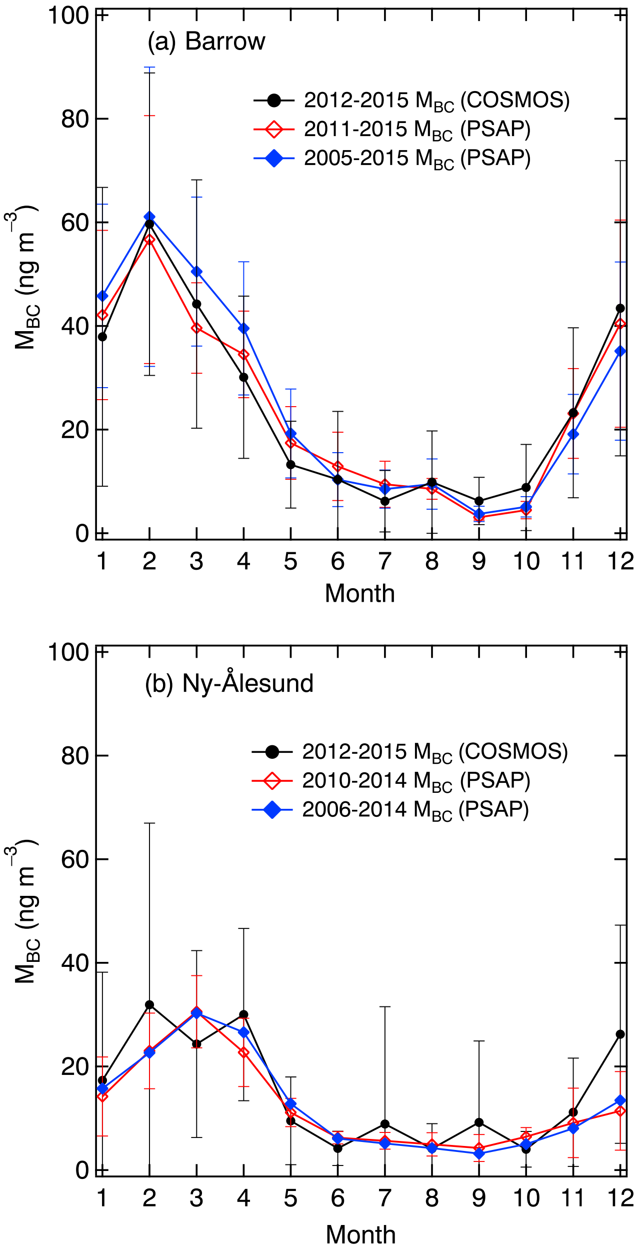

Figure 13. (a) Monthly mean M_{BC} (PSAP) at Barrow averaged over 5 years (2011–2015) and 10 years (2005–2015). (b) Monthly mean M_{BC} (PSAP) at Ny-Ålesund averaged over 5 years (2010–2014) and 8 years (2006–2015). Monthly mean M_{BC} (COSMOS) averaged over 2012–2015 is also shown in each panel. The vertical bars represent the standard deviations ($\pm 1\sigma$) of the monthly mean values.

(COSMOS) averaged over the 3 year period agreed with the M_{BC} (PSAP) values averaged over the 8 year period from April 2006 to December 2014 to within 15% (Figure 13b).

M_{BC} reached a maximum in winter and a minimum in summer, as shown by previous studies, although these studies did not critically evaluate the absolute values of M_{BC} [*Hirdman et al.*, 2010a, 2010b; *Eleftheriadis et al.*, 2009; *Sharma et al.*, 2013]. At Barrow, mean M_{BC} (COSMOS) was 38.4 ± 26.0 ng m^{-3} in winter and 9.3 ± 12.0 ng m^{-3} in summer between 2012 and 2015, whereas at Ny-Ålesund during those years, mean M_{BC} (COSMOS) was 22.3 ± 21.0 ng m^{-3} in winter and 6.2 ± 7.9 ng m^{-3} in summer.

During winter, daily M_{BC} (COSMOS) values between 20 and 30 ng m^{-3} were more frequent at Barrow than at Ny-Ålesund, where the distribution shifted to lower M_{BC} (COSMOS) values (section A11). In summer, the M_{BC} (COSMOS) distribution shifted to lower values with a mode of 5 ng m^{-3}, indicating more frequent occurrence of low BC loading. These seasonal variabilities in M_{BC} (COSMOS) have been attributed mainly to changes in air mass transport pathways from potential source regions, along with wet scavenging [*Browse et al.*, 2012; *Hirdman et al.*, 2010b; *Liu et al.*, 2011; *Sharma et al.*, 2013].

8. Comparison of M_{BC} (COSMOS) With Previous Measurements in the Arctic

To date, aethalometer and PSAP instruments have been widely used for continuous measurements of M_{BC} in the Arctic. *Hirdman et al.* [2010a, 2010b] reported M_{BC} values at Barrow and Ny-Ålesund based on measurements made by PSAP instruments, but they used different methods to derive M_{BC}. Because of the methodological differences, we denote M_{BC} values derived by these previous studies as M_{BC}^* (PSAP-PM$_1$) for Barrow and M_{BC}^* (PSAP-PM$_{10}$) for Ny-Ålesund in comparisons with our M_{BC} (PSAP) values, which were scaled by M_{BC} (COSMOS). The values of M_{BC}^* (PSAP-PM$_1$) and M_{BC}^* (PSAP-PM$_{10}$) were obtained from *Hirdman et al.* [2010a, Figure 2].

We compared monthly mean M_{BC}^* (PSAP-PM$_1$), M_{BC}^* (PSAP-PM$_{10}$), and M_{BC} (aethalometer) variations with monthly mean M_{BC} (COSMOS) and M_{BC} (PSAP) variations (Figure 14). The values of M_{BC} (aethalometer) at

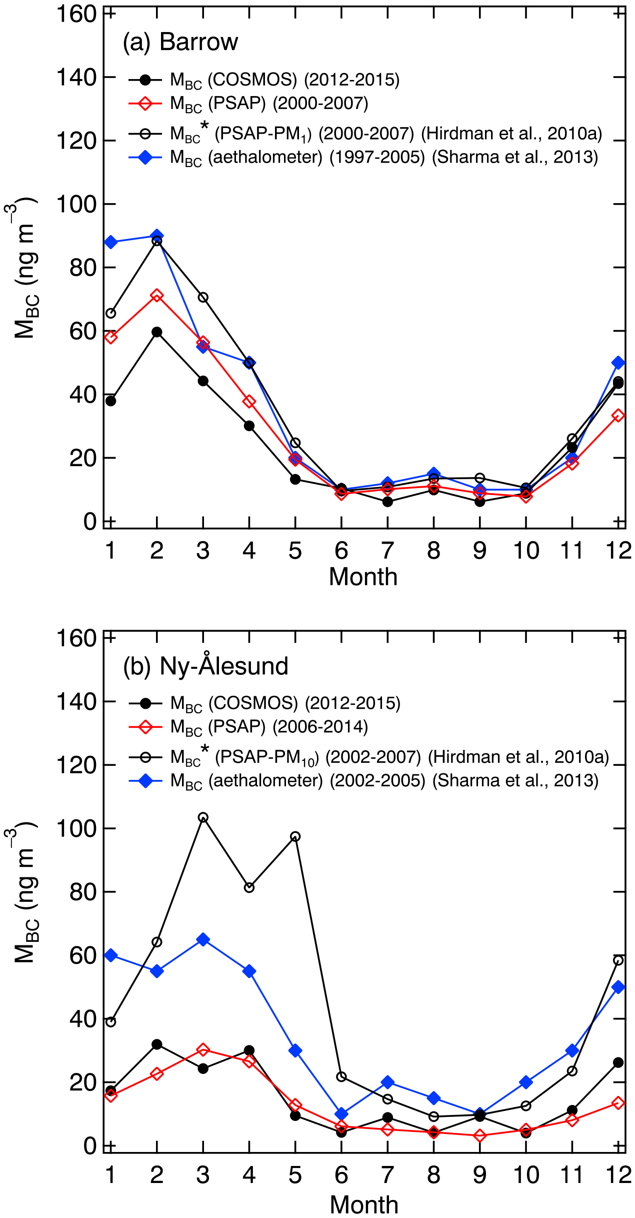

Figure 14. Comparisons of monthly mean M_{BC}* (PSAP-PM$_1$), M_{BC}* (PSAP-PM$_{10}$), and M_{BC} (aethalometer) with M_{BC} (COSMOS) and M_{BC} (PSAP) at (a) Barrow and (b) Ny-Ålesund. The M_{BC}* (PSAP-PM$_1$) data at Barrow (2000–2007) and M_{BC}* (PSAP-PM$_{10}$) data at Ny-Ålesund (2002–2007) are those obtained by *Hirdman et al.* [2010a], and the M_{BC} (aethalometer) data at Barrow (1997–2005) and Ny-Ålesund (2002–2005) are those obtained by *Sharma et al.* [2013].

Barrow were obtained from *Sharma et al.* [2013, Figure 6b]. The results for winter and summer are summarized in Table 4. At Barrow, in M_{BC}^* (PSAP-PM$_1$) and M_{BC} (PSAP) data collected during the same period (2002–2007), M_{BC}^* (PSAP-PM$_1$)/M_{BC} (PSAP) ratios were about 1.3 in both winter and summer (Figure 14a and Table 4). A MAC value of 10.0 m^2 g^{-1} was used to derive M_{BC}^* (PSAP-PM$_1$) [*Hirdman et al.*, 2010a, 2010b], whereas we calculated MAC to be 10.6 m^2 g^{-1} in this study. Thus, we estimate the difference between M_{BC}^* (PSAP-PM$_1$) and M_{BC} (PSAP) to be about 10–20%. In winter and summer, M_{BC} (aethalometer) differed from M_{BC} (PSAP) by a factor of about 1.3 and 1.2, respectively. This difference is much larger than the uncertainty of M_{BC} (PSAP).

At Ny-Ålesund, the M_{BC}^* (PSAP-PM$_{10}$)/M_{BC} (PSAP) ratios were about 3.2 and 3.6 in winter and summer, respectively (Figure 14b and Table 4). The M_{BC}^* (PSAP-PM$_{10}$) data were obtained during 2002–2007, whereas the M_{BC} (PSAP) data were obtained during 2006–2014, but the difference between M_{BC}^* (PSAP-PM$_{10}$) and M_{BC} (PSAP) far exceeds the temporal change in M_{BC} (PSAP) that would be expected from the long-term trend of about -0.56 ± 0.45 ng m^{-3} yr^{-1} derived at Barrow. A MAC value of 10.0 m^2 g^{-1} was used to derive M_{BC}^* (PSAP-PM$_{10}$), whereas in the present analysis, we obtained a MAC value of 12.5 m^2 g^{-1} (PM$_{10}$) for Ny-Ålesund. The large difference between M_{BC}^* (PSAP-PM$_{10}$) and M_{BC} (PSAP) cannot be explained only by the difference in the MAC values because they differ by a factor of only about 1.25. Thus, there must be other unidentified problems with the derivation of the PM$_{10}$ absorption coefficient at Ny-Ålesund prior to 2006.

The M_{BC} (aethalometer)/M_{BC} (PSAP) ratio was about 3.0 in winter and about 3.1 in summer. The values of M_{BC} (aethalometer) at Ny-Ålesund were taken from *Sharma et al.* [2013, Figure 6c]. The period of the M_{BC} (aethalometer) measurements (2002–2005) does not overlap the period of the M_{BC} (PSAP) measurements (2007–2014), but it is unlikely that these large ratios can be explained by the long-term trend in M_{BC} (PSAP), as discussed above.

The ratio of the M_{BC} (COSMOS) at Barrow to that at Ny-Ålesund in winter was about 1.77 ± 0.42. The corresponding M_{BC} (aethalometer) and M_{BC}^* (PSAP-PM$_1$) ratios were 0.81 ± 0.13 and 0.52 ± 0.23, respectively.

Table 4. Ratio of Scaled M_{BC} (PSAP) and M_{BC} Measured by Previous Studies by Using a PSAP (M_{BC}^* (PSAP)) and an Aethalometer (M_{BC} (Aethalometer)) at Barrow and Ny-Ålesund in Winter (November–April) and Summer (May–October)

	Barrow		Ny-Ålesund	
Season	M_{BC}^* (PSAP-PM$_1$)/M_{BC} (PSAP)	M_{BC} (aethalometer)/M_{BC} (PSAP)	M_{BC}^* (PSAP-PM$_{10}$)/M_{BC} (PSAP)	M_{BC} (aethalometer)/M_{BC} (PSAP)
Winter	1.28	1.28	3.18	2.98
Summer	1.26	1.19	3.63	3.09

Reliable ratios, such as those obtained by the present study, are important for improving our understanding of the spatial variability in M_{BC} in the Arctic.

9. Summary and Conclusion

Although long-term particle soot absorption photometer (PSAP) measurements of the light absorption coefficient (b_{abs}) (b_{abs} (PSAP)) have been reported by previous studies at Barrow, Alaska, and Ny-Ålesund, Spitsbergen, in the Arctic, those studies did not critically evaluate the effects on b_{abs} (PSAP) of aerosols coexisting with BC. Furthermore, they used different mass absorption cross section (MAC) values to convert b_{abs} to BC mass concentrations. We measured b_{abs} at these sites for about 3 years by using COSMOS (b_{abs} (COSMOS)), which uses a heated inlet to remove non-BC compounds, and then evaluated the performance of COSMOS for the measurement of BC mass concentrations (M_{BC} (COSMOS)) with particle diameters less than 1 μm (PM$_1$) at these sites.

We also showed by laboratory experiments with PSL particles that sea-salt aerosols caused M_{BC} (COSMOS) to be overestimated by about 2 ng m^{-3} on average under the conditions at Barrow and Ny-Ålesund. M_{BC} (COSMOS) derived by using MAC (COSMOS) obtained by our previous studies in Asia agreed to within 9%, with an uncertainty of 17%, with M_{EC} values measured by the thermal-optical transmittance technique at Barrow for 11 months (August 2012 to June 2013). Further, M_{BC} (COSMOS) values agreed to within 3%, with an uncertainty of 15%, with M_{BC} measured by a single particle soot photometer (SP2) near Ny-Ålesund for 3 days in winter 2013 during the ACCACIA aircraft campaign. These results indicate that at both sites, M_{BC} (COSMOS) was consistent and reliable.

We found that b_{abs} (PSAP) was highly correlated with b_{abs} (COSMOS). The high correlations enabled reliable estimation of M_{BC} (PSAP) from b_{abs} (PSAP). b_{abs} (PSAP) was systematically higher than b_{abs} (COSMOS) by 22% at Barrow (PM$_1$) and by 43% at Ny-Ålesund (PM$_{10}$). The higher b_{abs} (PSAP) than b_{abs} (COSMOS) is attributable to enhanced absorption by internal mixing of BC and additional light absorption by volatile light-absorbing aerosol species.

At Barrow, monthly mean M_{BC} (COSMOS) averaged over 3 years agreed to within 10% with M_{BC} (PSAP) averaged over 10 years. At Ny-Ålesund, the 3 year monthly mean M_{BC} (COSMOS) values agreed with M_{BC} (PSAP) values averaged over 8 years to within 15%. At Barrow, M_{BC} (COSMOS) reached a maximum of 38.4 ± 26.0 ng m^{-3} in winter and a minimum of 9.3 ± 12.0 ng m^{-3} in summer. At Ny-Ålesund, M_{BC} (COSMOS) was 22.3 ± 21.0 ng m^{-3} in winter and 6.2 ± 7.9 ng m^{-3} in summer during 2012–2015.

We estimated the linear trend of M_{BC} (PSAP) values obtained at Barrow during 1998–2015 by linear regression and the Markov chain Monte Carlo methods. The seasonally averaged M_{BC} (PSAP) generally decreased in winter and summer at a rate of about 0.55 ± 0.30 ng m^{-3} yr^{-1}. However, the absolute values of the rates are highly uncertain, partly owing to the large year-to-year variability of M_{BC} (PSAP) values.

At Ny-Ålesund, M_{BC}^* (PSAP-PM$_{10}$) values were systematically greater than M_{BC} (PSAP) values by a factor of 3.2 and 3.6 in winter and summer, respectively. M_{BC} (aethalometer) values were greater than M_{BC} (PSAP) values by a factor of 1.3 at Barrow in both winter and summer and of about 3.0 and 3.1 at Ny-Ålesund in winter and summer, respectively. We analyzed the causes of the inconsistency in the previously reported M_{BC} values in the Arctic.

The accuracy of M_{BC} (COSMOS) has been critically assessed by this study, and we anticipate that M_{BC} (COSMOS) will continue to be a reliable reference value for M_{BC} at Barrow and Ny-Ålesund in the Arctic.

Appendix A

A1. Measurements of b_{abs} and b_{sca} at Barrow and Ny-Ålesund

In this Appendix, we describe the measurement method of b_{abs} by using PSAP and CLAP at Barrow and Ny-Ålesund. The ambient air was aspirated at a flow rate of about 0.9 L min^{-1} at STP to measure b_{abs}. Unlike the PSAP, the CLAP uses a solenoid valve to cycle through eight sample filter spots and two reference spots, which facilitates field observations, particularly in remote locations.

b_{sca} at $\lambda = 550$ nm was measured with integrating nephelometers at Barrow (PM_1 and PM_{10}) and Ny-Ålesund. Detailed descriptions of the measurements, instrument calibration, and uncertainty analysis are presented elsewhere [*Anderson and Ogren*, 1998; *Anderson et al.*, 1999; *Sheridan et al.*, 2001]. The overall uncertainty of b_{sca} averaged over 1 min, accounting for instrumental noise, drift in calibration, Rayleigh scattering of air, and blocking of near-forward scattering light (truncation), was less than 10% [*Sheridan et al.*, 2001]. The uncertainty of b_{abs} (PSAP) was estimated to be about 20% for the 1 h average at midlatitudes (35°N–45°N), taking account of instrumental noise, calibration of PSAP following *Bond et al.* [1999], and unit-to-unit variability [*Sherman et al.*, 2015].

The PSAP and nephelometers at Barrow were equipped with switchable PM_1 and PM_{10} impactors for particle size selection. The PM_1 and PM_{10} size ranges were alternated every 30 min (twice each hour). We therefore used b_{abs} values obtained by the PSAP during the last 30 min of each hour for the comparison with the COSMOS measurements at Barrow in this study. Data were further screened to avoid any local contamination; only data collected when the wind direction was from the clean air sector, from 0 to 130°, were included.

At Ny-Ålesund, measurements of b_{abs} at 532 nm were also carried out at about 10 m above the ground by using a custom-built PSAP until November 2012. The custom-built PSAP was replaced with a new PSAP in December 2012. The b_{abs} values obtained by the new PSAP were larger than those obtained by the custom-built PSAP by a factor of about 1.52 on average. The b_{abs} (PSAP) data obtained after December 2012 were corrected for this bias. These b_{abs} (PSAP) values were also adjusted to 550 nm as described in section 3.

A2. Measurements of the Mass Concentration of Sea Salt at Barrow and Ny-Ålesund

For measurement of the $M_{s\text{-}s}$ at Barrow, ambient air samples were collected onto filters after particle-size selection by PM_1 and PM_{10} impactors through an inlet mounted 10 m above the ground from October 1997 to December 2009. The chemical composition of the collected aerosols, including Na^+ and Cl^-, was analyzed by ion chromatography. Depending on the season and the aerosol loading, filter samples were collected at 1 to 4 day intervals at Barrow. *Quinn et al.* [2002] have described the sampling and measurement analysis at Barrow in detail. We estimated $M_{s\text{-}s}$ from the Na^+ concentration, and we also took into account the Cl^- concentration to minimize the effect of the loss of Cl^- owing to the release of HCl from the sea-salt aerosol. Other components such as sulfate that are not always present in sea-salt aerosols at the standard seawater ratio also add to the uncertainty in the estimation of $M_{s\text{-}s}$ with equation (7).

At Ny-Ålesund, ambient air samples containing sea-salt particles were collected daily from January 2012 to December 2014 as part of a cooperative program for monitoring and evaluation of long-range transmission of air pollutants in Europe (European Monitoring and Evaluation Programme) by using a filter pack sampler mounted 2 m above the ground. No impactor was used to restrict the size of the particles for $M_{s\text{-}s}$ measurement at Ny-Ålesund, but for simplicity, we refer to these data as PM_{10} in our comparison, despite the fact that the resulting $M_{s\text{-}s}$ values might be larger than $M_{s\text{-}s}$ (PM_{10}) values.

Hjellbrekke and Fjæraa [2009] have described the detailed sample collection and analysis procedures. $M_{s\text{-}s}$ in the submicrometer size range at Ny-Ålesund was deduced by assuming the value of f_{PM1} (=PM_1/PM_{10} ratio) of $M_{s\text{-}s}$ measured at Barrow. At Barrow, f_{PM1} varied between 0.08 and 0.77 during 1997–2009. The use of the measured values of $M_{s\text{-}s}$ may result in the overestimation of $M_{s\text{-}s}$ (PM_1) at Ny-Ålesund. Such overestimation would have little influence on the conclusion derived from this analysis, however.

A3. Measurements of M_{EC} at Barrow

The samples were collected outdoors on a sampling platform 10 m above ground level at the North Slope of Alaska Atmospheric Radiation Measurement Facility at Barrow. Filters were heated to 500°C for 12 h prior to

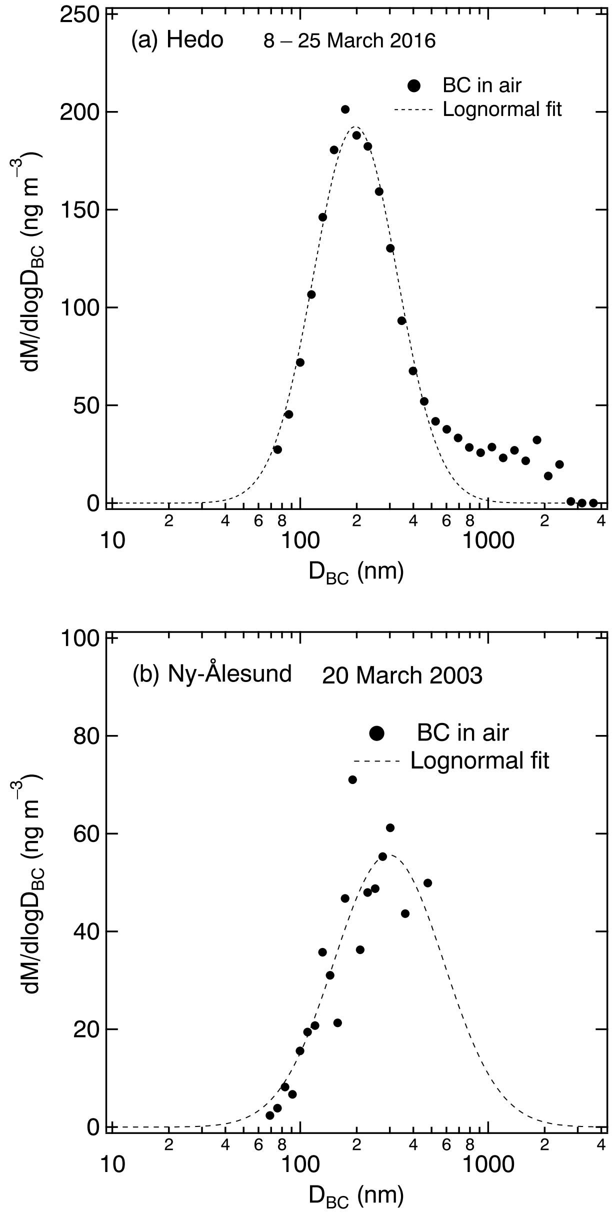

Figure A1. (a) Mean mass size distribution of BC particles measured by SP2 between 8 and 25 March 2016 at Hedo, Okinawa. The dashed line shows the fitted lognormal function. (b) Same as Figure A1a but of airborne SP2 measurements made near Zeppelin station, Ny-Ålesund, on 20 March 2013, during the ACCACIA campaign.

the sampling and stored in aluminum foil packets; they were kept in a freezer both before and after sampling. Each filter sampling period was approximately 7 days long during the entire observation period between August 2012 and June 2013. Measurements of M_{EC} were made in two combustion phases. In the first phase, each quartz fiber filter containing samples of particulate matter was heated to 870°C in an oxygen-free helium atmosphere and then heated to 900°C in the presence of 2% oxygen. In the second heating phase, EC and carbon produced by pyrolysis of organic carbon (OC) were converted to CO_2. CO_2 was then converted to methane and measured by a flame ionization detector. To correct for the pyrolytic conversion of OC to EC, the transmittance of a pulsed diode laser beam at 670 nm through a quartz fiber filter was monitored during the sample analysis. Calibration of the TOT analyzer was carried out with a sucrose standard after every 10 samples. The blank value (0.18 μg cm^{-2} of OC) was subtracted from all sample measurements. The M_{EC} values were not affected by the blank subtraction [*Barrett et al.*, 2015]. The M_{EC} values are given in units of ng m^{-3} STP.

A4. Measurements of the Size Distribution of BC at Hedo and Near Ny-Ålesund

1. Hedo

To determine the contribution of BC aerosol particles with diameters larger than 1 μm to total M_{BC}, we used the BC mass size distribution measured by an SP2 at the remote site of Hedo (26.9°N, 128.3°E) on Okinawa Island, Japan, during 17 days in March 2016 (Figure A1a). Hedo is located downstream of China [*Kondo et al.*, 2011c]. BC mass concentrations below the detection limit of the SP2 (around 75 nm) were estimated by extrapolating a lognormal function fitted to the BC mass size distribution. Mean M_{BC} was 128.8 ng m^{-3} between 0 and 4000 nm (PM$_4$) and 10.0 ng m^{-3} between 1000 and 4000 nm. On average, the ratio of M_{BC} above 1 μm in diameter to total M_{BC} was 0.08 (8%).

2. Ny-Ålesund

The BC mass size distribution in airborne SP2 measurements at an altitude of about 500 m near Zeppelin station, Ny-Ålesund, on 20 March 2013, is shown in Figure A1b. BC mass concentrations above the

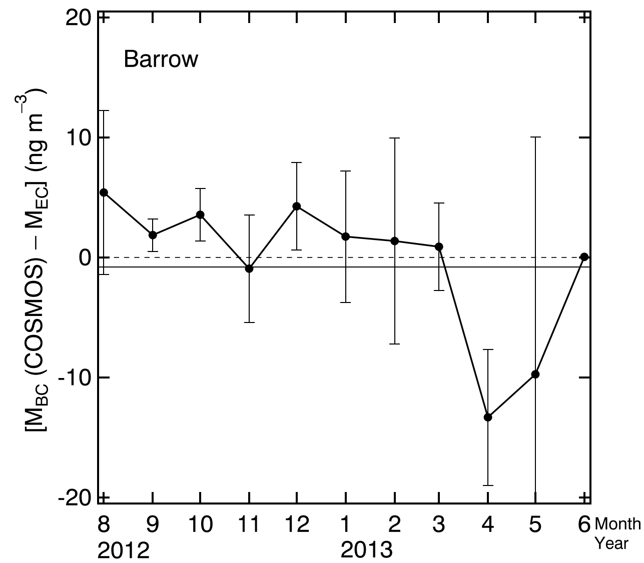

Figure A2. Time series of the difference between the monthly mean values of M_{BC} (COSMOS) and M_{EC} at Barrow from August 2012 to June 2013. The vertical bars represent the standard deviations (±1σ) of the monthly mean values, and the annual mean value is shown by the dashed horizontal line.

detection range of the SP2 measurements of 477 nm were estimated from a lognormal function fitted to the BC mass size distribution up to 1000 nm. The contributions of BC mass concentrations between 478 nm and 1000 nm to M_{BC} (SP2) for PM_1 were estimated to be in the range of 8.7–17.7% between 20 and 23 March 2013 with a mean contribution of about 15%.

A5. Seasonal Variation of the Difference Between M_{BC} (COSMOS) and M_{EC} at Barrow

Figure A2 presents the monthly mean values of the difference between M_{BC} (COSMOS) and M_{EC} at Barrow from August 2012 to June 2013. The M_{BC} (COSMOS)-M_{EC} difference was generally lower than 5 ng m^{-3} for most months except April and May 2013. However, no distinct seasonal variation in the monthly mean difference between M_{BC} (COSMOS) and M_{EC} is apparent.

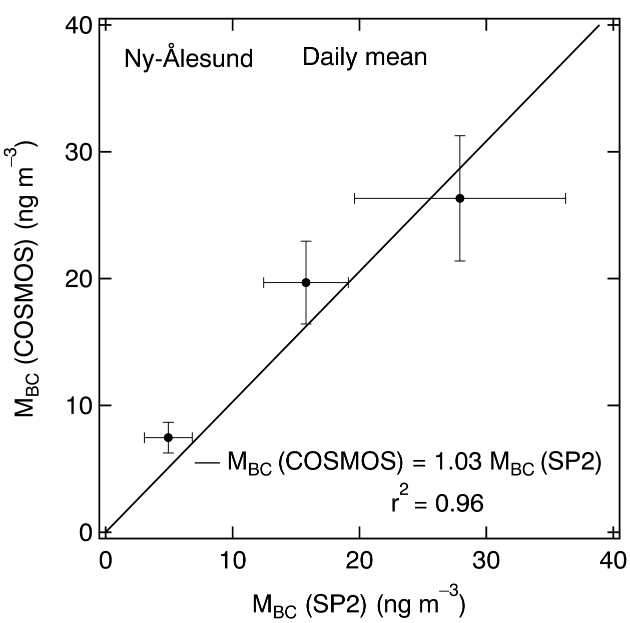

Figure A3. Correlation between daily mean M_{BC} (COSMOS) and M_{BC} (SP2) values measured during the ACCACIA campaign near Ny-Ålesund.

A6. Comparison of M_{BC} (COSMOS) and M_{BC} (SP2) at Ny-Ålesund

We compared the daily mean M_{BC} (COSMOS) with M_{BC} (SP2) values linearly interpolated to 474 m altitude and present the results in Figure A3. The daily mean M_{BC} (COSMOS) and M_{BC} (SP2) agreed to within about 3% (slope = 1.03, r^2 = 0.96) with an uncertainty of about 15%, although the statistical reliability is limited owing to the small number of M_{BC} (SP2) measurements.

A7. Daily and Monthly Variations of the Single Scattering Albedo at Barrow and Ny-Ålesund

Time series plots of daily and monthly mean variations of the single scattering albedo (SSA) from

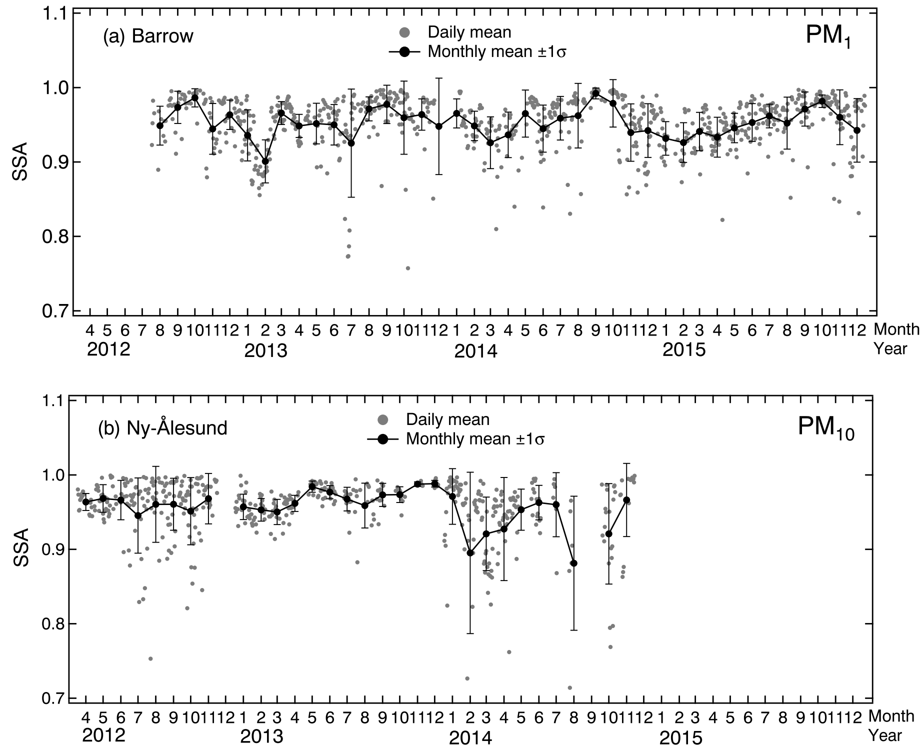

Figure A4. (a) Daily and monthly mean values of single scattering albedo (SSA) for PM$_1$ at Barrow from 2012 to 2015. (b) Same as Figure A4a but at Ny-Ålesund for PM$_{10}$ during 2012–2014.

hourly data at Barrow (PM$_1$) and Ny-Ålesund (PM$_{10}$) are shown Figure A4. At Barrow, SSA showed considerable day-to-day variability, particularly during winter, whereas at Ny-Ålesund, conspicuous variability was not seen, although episodically low SSA values were observed there in both winter and summer.

The amplitude of the seasonal variation of SSA was stronger at Barrow than at Ny-Ålesund. At Barrow, the mean wintertime SSA value (0.94 ± 0.03) in winter was lower than the summertime mean (0.96 ± 0.04). This wintertime SSA value is very similar to the value of 0.94 derived by *Delene and Ogren* [2002] for March–May during 1997–2000. At Ny-Ålesund, the mean wintertime SSA value of 0.95 ± 0.05 was higher than the wintertime mean at Barrow, but the summertime mean (0.96 ± 0.04) was similar to that at Barrow.

A8. Comparison of M_{BC} (COSMOS) and M_{BC} (PSAP) at Barrow and Ny-Ålesund

A8.1. Difference Between Monthly Mean M_{BC} (COSMOS) and M_{BC} (PSAP)

Time series of the difference between monthly mean M_{BC} (COSMOS) and M_{BC} (PSAP) at Barrow (2012–2015) and at Ny-Ålesund (2012–2014) are presented in Figure A5. Although this difference, M_{BC} (COSMOS)-M_{BC} (PSAP), varied greatly from year to year, the variation was not systematic at these sites during the study period. The difference was generally less than 10 ng m^{-3} at both sites, and the standard deviation of the difference was about 4.7 ng m^{-3} at Barrow and 3.8 ng m^{-3} at Ny-Ålesund. The maximum year-to-year variability of MAC (PSAP) was about ±20% at Barrow. This value is a measure of the year-to-year stability of the M_{BC} (PSAP) measurements in the Arctic and partly accounts for the difference between the monthly mean values of M_{BC} (COSMOS) and M_{BC} (PSAP).

A8.2. Scatterplot of Monthly Mean M_{BC} (COSMOS) and M_{BC} (PSAP)

We examined the correlation between monthly mean M_{BC} (COSMOS) and M_{BC} (PSAP) values at Barrow and Ny-Ålesund to visualize the degree to which individual data points deviated from the average correlation,

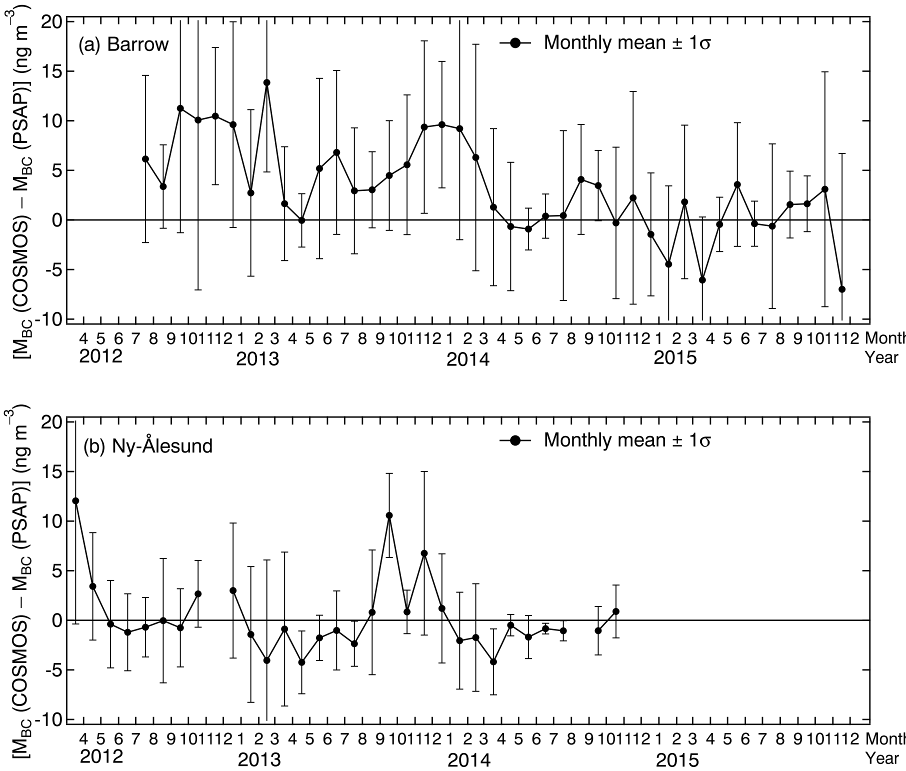

Figure A5. (a) Time series of the difference between monthly mean values of M_{BC} (COSMOS) and M_{BC} (PSAP) at Barrow during 2012–2015. The vertical bars represent the standard deviations (±1σ) of the monthly mean values. (b) Same as Figure A5a but at Ny-Ålesund for PM_{10} during 2012–2014.

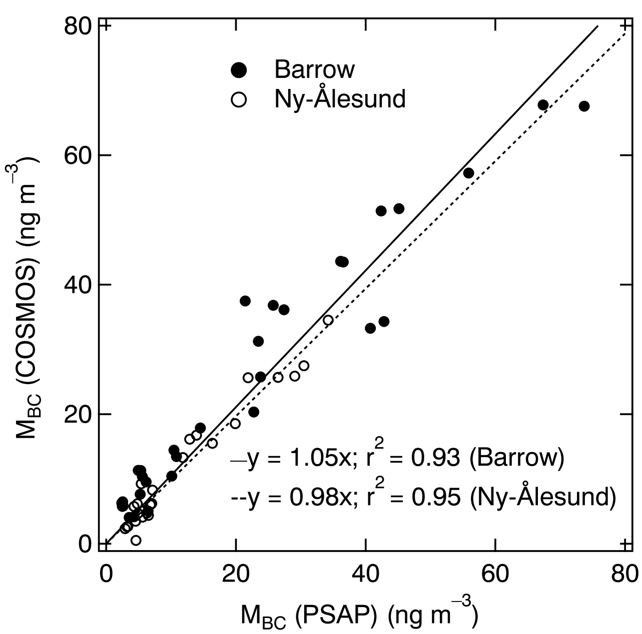

Figure A6. Correlations between monthly mean M_{BC} (COSMOS) and M_{BC} (PSAP) values at Barrow and Ny-Ålesund. We excluded the monthly means of M_{BC} (COSMOS) and M_{BC} (PSAP) for months with less than 17 daily data points.

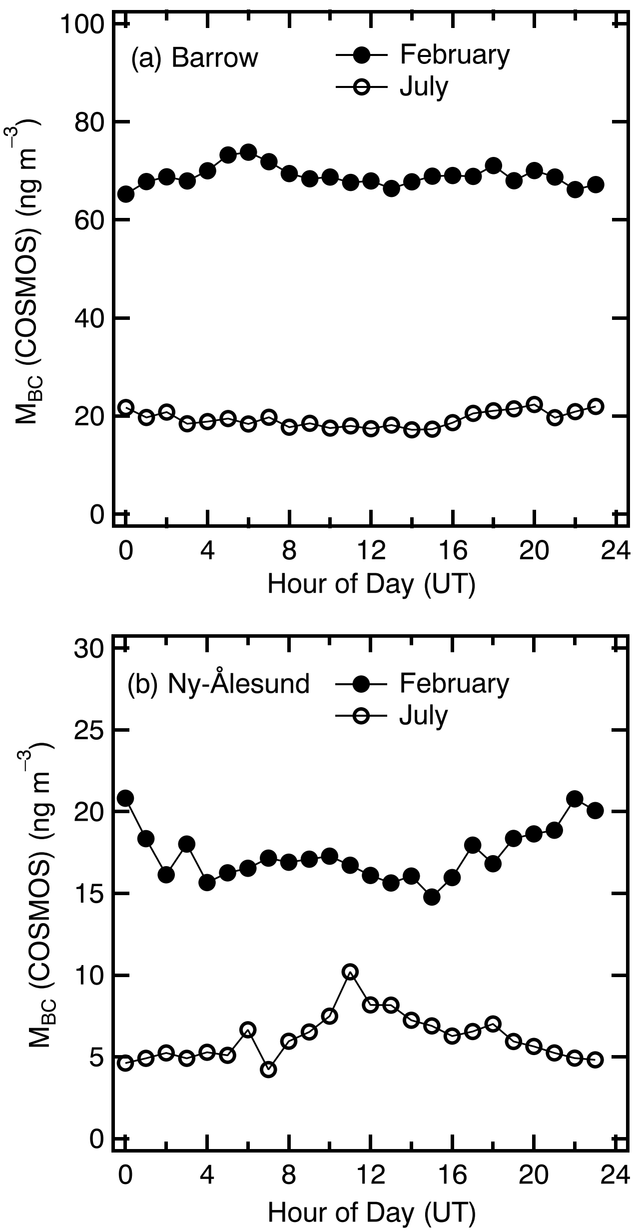

Figure A7. Diurnal variations of M_{BC} (COSMOS) values averaged over February and July 2013 at (a) Barrow and (b) Ny-Ålesund.

as shown in Figure A6. Monthly mean M_{BC} (COSMOS) and M_{BC} (PSAP) values were well correlated ($r^2 = 0.96$ at Barrow and 0.95 at Ny-Ålesund), as expected given the correlations between b_{abs} (PSAP) and b_{abs} (COSMOS). The average slope was 1.05 at Barrow and 0.98 at Ny-Ålesund, as a result of the scaling.

A9. Diurnal Variation of M_{BC} at Barrow and Ny-Ålesund

Monthly mean diurnal variations of M_{BC} (COSMOS) at Barrow and Ny-Ålesund in February and July 2013 are shown in Figure A7. These months were chosen as representative of the winter and summer seasons, respectively. At both sites, the amplitude of the diurnal variation in M_{BC} (COSMOS) was generally smaller in July than in February, partly reflecting the seasonal variation in M_{BC} (COSMOS). Overall, the monthly mean diurnal variation of M_{BC} (COSMOS) was generally less than 10% of the daily mean in all months. Similarly, *Sharma et al.* [2002] and *Eleftheriadis et al.* [2009] reported weak diurnal variability in M_{BC} at Ny-Ålesund. The absence of diurnal variability in M_{BC} (COSMOS) suggests that the influence of localized BC emissions on the measured M_{BC} was small; however, anthropogenic activities have been observed to vary diurnally in more populated areas [e.g., *Sahu et al.*, 2011]. In addition, if very high concentrations of BC are confined within the relatively shallow atmosphere near

Table A1. Trends of Seasonally Averaged M_{BC} (PSAP) Between 1998 and 2015 at Barrow[a]

	Markov Chain Monte Carlo Method	Least-Squares Fit	
Month	Slope (ng m^{-3} yr^{-1}) ±1σ	Slope (ng m^{-3} yr^{-1}) ±1σ	r^2
December–February	−1.04 ± 0.64	−1.04 ± 0.75	0.11
March–May	−0.94 ± 0.79	−0.37 ± 0.38	0.06
June–August	−0.43 ± 0.27	−0.41 ± 0.19	0.24
September–November	−0.44 ± 0.29	−0.55 ± 0.16	0.43

[a]The linear trends and their standard deviations (±1σ) were estimated by a regression analysis performed by using the Markov chain Monte Carlo method. The linear trends estimated by least squares fitting are also shown, together with their ±1σ and r^2 values.

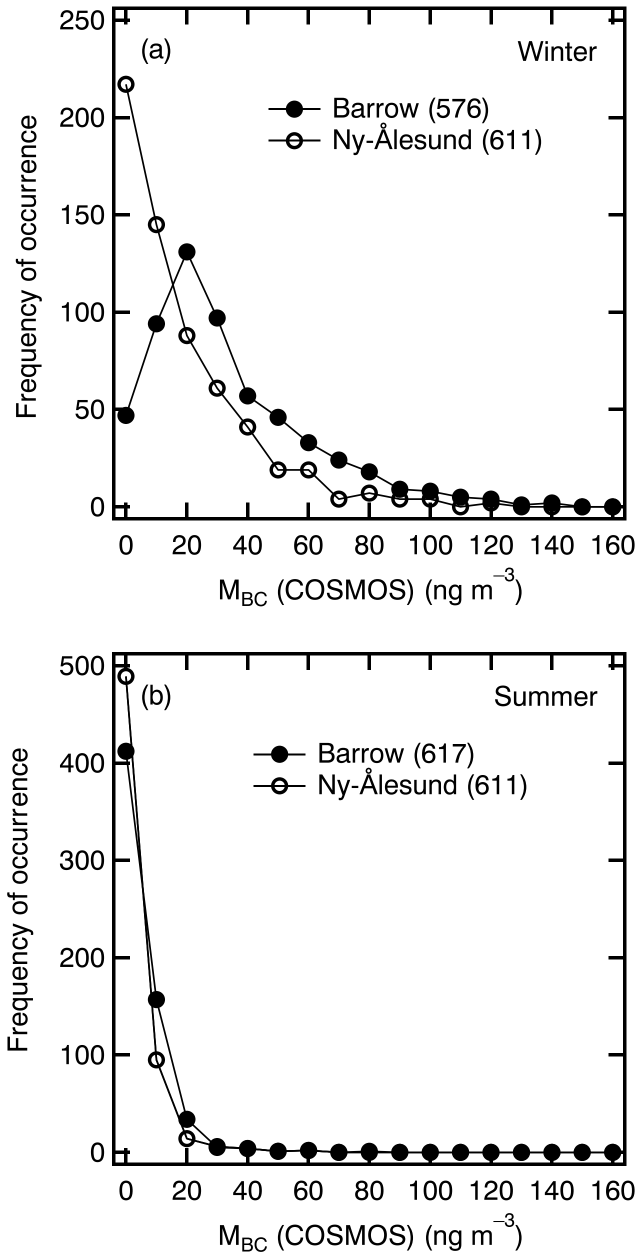

Figure A8. Frequency distributions of daily mean M_{BC} (COSMOS) at Barrow and Ny-Ålesund in (a) winter (November–April) and (b) summer (May–October) from 2012 to 2015. The number of data points in each season at each site is shown in parentheses.

the measurement sites, diurnal variations of BC might be associated with variations in the thickness of the planetary boundary layer.

A10. Long-Term Trends of M_{BC} (PSAP)

We also estimated long-term trends by performing a regression analysis of M_{BC} (PSAP) at Barrow against time by the Bayesian statistical method [e.g., *Hoff*, 2009] in addition to the LS method. Under this mathematical formulation, the probability distribution of the linear trend (slope) was evaluated as a posterior distribution of M_{BC} (PSAP). The expected value of the slope and its uncertainty were evaluated as the mean and standard deviation, respectively, of ~2×10^5 sampling points over the slope-intercept space obtained by the Markov chain Monte Carlo (MCMC) method.

We applied this method to time series of M_{BC} (PSAP) values obtained during 1998–2015 at Barrow and averaged over 3 month periods. The resulting slopes and their $\pm 1\sigma$ values are summarized in Table A1. For comparison, the results obtained by the LS method are also summarized in Table A1. In general, the slopes obtained by least squares fitting were similar to those obtained by the MCMC method, but the slopes for March–May differed between the two methods.

A11. Frequency Distribution of M_{BC} at Barrow and Ny-Ålesund

The frequency distributions of the daily mean M_{BC} (COSMOS) values during winter and summer at Barrow and Ny-Ålesund are presented in Figure A8. During winter, values of M_{BC} (COSMOS) of 20–30 ng m^{-3} were more frequent at Barrow than at Ny-Ålesund, where the distribution was shifted to lower M_{BC} (COSMOS) values. The frequency distributions of M_{BC} (COSMOS) at the two sites had long thin tails, which extended to more than 100 ng m^{-3}, in winter. During summer, the frequency distributions of M_{BC} (COSMOS) were similar at the two sites. The M_{BC} (COSMOS) distribution was skewed toward lower values, with a mode at 5 ng m^{-3}, indicating more frequent occurrence of low BC loadings. The frequency distributions of M_{BC} (COSMOS) were much narrower at lower M_{BC} values in summer compared with those in winter. The seasonal variation in M_{BC} (COSMOS) is mainly attributable to changes in transport pathways and the degree of wet deposition of BC during transport. It is often difficult for transport models to predict precisely trajectories of individual air parcels reaching the observation sites at given times. Comparison of the occurrence frequencies observed by this study and those calculated by numerical models would be useful for statistical evaluation of the transport processes included in the models. Such a comparison was made for Asia by *Kondo et al.* [2011c].

Acknowledgments
We thank NOAA personnel for reliably carrying out the observations by PSAP, nephelometer, and COSMOS instruments at Barrow. We also thank the staff of the Norwegian Polar Institute for reliably performing the COSMOS measurements at Zeppelin station, Ny-Ålesund. This work was supported by the Ministry of Education, Culture, Sports, Science, and Technology (MEXT), the Global Environment Research Fund of the Japanese Ministry of the Environment (A-1101, 2-1403, and 2-1703), the Japan Society for the Promotion of Science (JSPS) KAKENHI grants (JP12J06736, JP23221001, and JP16H01770), the GRENE Arctic Climate Change Research Project, and the Arctic Challenge for Sustainability (ArCS) project. This is Pacific Marine Environmental Laboratory (PMEL) contribution number 4552. We thank the anonymous reviewers for their constructive comments and suggestions. The data used in this study are available upon request from the authors. (kondo.yutaka@nipr.ac.jp).

References

Anderson, T. L., and J. A. Ogren (1998), Determining aerosol radiative properties using the TSI 3563 integrating nephelometer, *Aerosol Sci. Technol.*, *29*, 57–69.

Anderson, T. L., D. S. Covert, J. D. Wheeler, J. M. Harris, K. D. Perry, B. E. Trost, D. J. Jaffe, and J. A. Ogren (1999), Aerosol backscatter fraction and single scattering albedo: Measured values and uncertainties at a coastal station in the Pacific Northwest, *J. Geophys. Res.*, *104*(D21), 26,793–26,807, doi:10.1029/1999JD900172.

Barrett, T. E., E. M. Robinson, S. Usenko, and R. J. Sheesley (2015), Source contributions to wintertime elemental and organic carbon in the western Arctic based on radiocarbon and tracer apportionment, *Environ. Sci. Technol.*, *49*, 11,631–11,639.

Barrie, L. A., and M. J. Barrie (1990), Chemical components of lower tropospheric aerosols in the high Arctic: Six years of observations, *J. Atmos. Chem.*, *11*, 211–226.

Birch, M. E., and R. A. Cary (1996), Elemental carbon-based method for monitoring occupational exposures to particulate diesel exhaust, *Aerosol Sci. Technol.*, *25*, 221–241.

Bodhaine, B. A. (1995), Aerosol absorption measurements at Barrow, Mauna Loa and the south pole, *J. Geophys. Res.*, *100*(D5), 8967–8975, doi:10.1029/95JD00513.

Bond, T. C., T. L. Anderson, and D. Campbell (1999), Calibration and inter-comparison of filter based measurements of visible light absorption by aerosols, *Aerosol Sci. Technol.*, *30*, 582–600.

Bond, T. C., et al. (2013), Bounding the role of black carbon in the climate system: A scientific assessment, *J. Geophys. Res. Atmos.*, *118*, 5380–5552, doi:10.1002/jgrd.50171.

Brock, C. A., et al. (2011), Characteristics, sources, and transport of aerosols measured in spring 2008 during the Aerosol, Radiation, and Cloud Processes Affecting Arctic Climate (ARCPAC) project, *Atmos. Chem. Phys.*, *11*, 2423–2453.

Browse, J., K. S. Carslaw, S. Arnold, K. J. Pringle, and O. Boucher (2012), The scavenging processes controlling the seasonal cycle in Arctic sulphate and black carbon aerosol, *Atmos. Chem. Phys.*, *12*, 6775–6798.

Collaud Coen, M., et al. (2013), Aerosol decadal trends—Part 1: In-situ optical measurements at GAW and IMPROVE stations, *Atmos. Chem. Phys.*, *13*, 869–894.

Delene, D. J., and J. A. Ogren (2002), Variability of aerosol optical properties at four North American surface monitoring sites, *J. Atmos. Sci.*, *59*, 1135–1150.

Eleftheriadis, K., S. Vratolis, and S. Nyeki (2009), Aerosol black carbon in the European Arctic: Measurements at Zeppelin station, Ny-Ålesund, Svalbard from 1998–2007, *Geophys. Res. Lett.*, *36*, L02809, doi:10.1029/2008GL035741.

Flanner, M. G., C. S. Zender, J. T. Randerson, and P. J. Rasch (2007), Present day climate forcing and response from black carbon in snow, *J. Geophys. Res.*, *112*, D11202, doi:10.1029/2006JD008003.

Hirdman, D., H. Sodemann, S. Eckhardt, J. F. Burkhart, A. Jefferson, T. Mefford, P. K. Quinn, S. Sharma, J. Ström, and A. Stohl (2010a), Source identification of short-lived air pollutants in the Arctic using statistical analysis of measurement data and particle dispersion model output, *Atmos. Chem. Phys.*, *10*, 669–693.

Hirdman, D., J. F. Burkhart, H. Sodemann, S. Eckhardt, A. Jefferson, P. K. Quinn, S. Sharma, J. Ström, and A. Stohl (2010b), Long-term trends of black carbon and sulphate aerosol in the Arctic: Changes in atmospheric transport and source region emissions, *Atmos. Chem. Phys.*, *10*, 9351–9368.

Hjellbrekke, A.-G., and A. M. Fjæraa (2009), *Data Report 2007: Acidifying and Eutrophying Compounds and Particulate Matter, EMEP/CCC Report 1/2009*, Norwegian Institute for Air Research, Kjeller, Norway.

Hoff, P. D. (2009), *A First Course in Bayesian Statistical Methods*, pp. 270, Springer, London.

Holland, H. D. (1978), *The Chemistry of the Atmosphere and Oceans*, pp. 369, John Wiley, New York.

Irwin, M., Y. Kondo, N. Moteki, and T. Miyakawa (2013), Evaluation of a heated-inlet for calibration of the SP2, *Aerosol Sci. Technol.*, *47*, 895–905.

Kondo, Y. K. (2015), Effects of black carbon on climate: Advances in measurement and modeling, *Monogr. Environ. Earth Planets*, *3*, 1–85.

Kondo, Y., et al. (2009), Stabilization of the mass absorption cross section of black carbon for filter-based absorption photometry by the use of a heated inlet, *Aerosol Sci. Technol.*, *43*, 741–756.

Kondo, Y., et al. (2011a), Emissions of black carbon, organic, and inorganic aerosols from biomass burning in North America and Asia in 2008, *J. Geophys. Res.*, *116*, D08204, doi:10.1029/2010JD015152.

Kondo, Y., L. Sahu, N. Moteki, F. Khan, N. Takegawa, X. Liu, M. Koike, and T. Miyakawa (2011b), Consistency and traceability of black carbon measurements made by laser-induced incandescence, thermal-optical transmittance, and filter-based photo-absorption techniques, *Aerosol Sci. Technol.*, *45*, 295–312.

Kondo, Y., N. Oshima, M. Kajino, R. Mikami, N. Moteki, N. Takegawa, R. L. Verma, Y. Kajii, S. Kato, and A. Takami (2011c), Emissions of black carbon in East Asia estimated from the observations at a remote site in the East China Sea, *J. Geophys. Res.*, *116*, D16291, doi:10.1029/2011JD015637.

Kondo, Y., N. Moteki, S. Ohata, N. Oshima, M. Koike, Y. Shibano, N. Takegawa, and K. Kita (2016), Effects of wet deposition on the abundance and size distribution of black carbon in East Asia, *J. Geophys. Res. Atmos.*, *121*, 4961–4712, doi:10.1002/2015JD024479.

Krecl, P., J. Ström, and C. Johansson (2007), Carbon content of atmospheric aerosols in a residential area during the wood combustion season in Sweden, *Atmos. Environ.*, *41*, 6974–6985.

Lack, D. A., H. Moosmüller, G. R. McMeeking, R. K. Chakrabarty, and D. Baumgardner (2014), Characterizing elemental, equivalent black, and refractory black carbon aerosol particles: A review of techniques, their limitations and uncertainties, *Anal. Bioanal. Chem.*, *406*, 99–122, doi:10.1007/s00216-013-7402-3.

Liu, D., et al. (2010), Single particle characterization of black carbon aerosols at a tropospheric alpine site in Switzerland, *Atmos. Chem. Phys.*, *10*, 7389–7407.

Liu, D., et al. (2015), The importance of Asia as a source of black carbon to the European Arctic during springtime 2013, *Atmos. Chem. Phys.*, *15*, 11,537–11,555.

Liu, J., S. Fan, L. Horowitz, and H. Levy (2011), Evaluation of factors controlling long-range transport of black carbon to the Arctic, *J. Geophys. Res.*, *116*, D04307, doi:10.1029/2010JD015145.

Matsui, H., et al. (2011), Seasonal variation of the transport of black carbon aerosol from the Asian continent to the Arctic during the ARCTAS aircraft campaign, *J. Geophys. Res.*, *116*, D05202, doi:10.1029/2010JD015067.

McMeeking, G. R., et al. (2010), Black carbon measurements in the boundary layer over western and northern Europe, *Atmos. Chem. Phys.*, *10*, 9393–9414.

McNaughton, C. S., et al. (2011), Absorbing aerosol in the troposphere of the western Arctic during the 2008 ARCTAS/ARCPAC airborne field campaigns, *Atmos. Chem. Phys.*, *11*, 7561–7582.

Miyakawa, T., N. Oshima, F. Taketani, Y. Komazaki, A. Yoshino, A. Takami, Y. Kondo, and Y. Kanaya (2016), Alteration of the microphysical properties of black carbon through transport in the boundary layer in East Asia, *Atmos. Chem. Phys. Discuss.*, doi:10.5194/acp-2016-570.

Miyazaki, Y., Y. Kondo, L. K. Sahu, J. Imaru, N. Fukushima, and A. Kanno (2008), Performance of a newly designed continuous soot monitoring system (COSMOS), *J. Environ. Monit.*, *10*, 1195–1201.

Moteki, N., and Y. Kondo (2008), Method to measure time-dependent scattering cross-section of particles evaporating in a laser beam, *J. Aerosol Sci.*, *39*, 348–364.

Moteki, N., and Y. Kondo (2010), Dependence of laser-induced incandescence on physical properties of black carbon aerosols: Measurements and theoretical interpretation, *Aerosol Sci. Technol.*, *44*, 663–675.

Moteki, N., Y. Kondo, T. Nakayama, K. Kita, L. K. Sahu, T. Ishigai, T. Kinase, and Y. Matsumi (2010), Radiative transfer modeling of filter-based measurements of light absorption by particles: Importance of particle size dependent penetration depth, *J. Aerosol Sci.*, *41*, 401–412.

Moteki, N., Y. Kondo, N. Oshima N. Takegawa, M. Koike, K. Kita, H. Matsui, and M. Kajino (2012), Size dependence of wet removal of black carbon aerosols during transport from the boundary layer to the free troposphere, *Geophys. Res. Lett.*, *39*, L13802, doi:10.1029/2012GL052034.

Ogren, J. A. (2010), Comments on "Calibration and inter-comparison of filter-based measurements of visible light absorption by aerosols", *Aerosol Sci. Technol.*, *44*, 589–591.

Ohata, S., J. P. Schwarz, N. Moteki, M. Koike, A. Takami, and Y. Kondo (2016), Hygroscopicity of materials internally mixed with black carbon measured in Tokyo, *J. Geophys. Res. Atmos.*, *121*, 362–381, doi:10.1002/2015JD024153.

Petzold, A., et al. (2013), Recommendations for reporting "black carbon" measurements, *Atmos. Chem. Phys.*, *13*, 8365–8379.

Quinn, P. K., T. L. Miller, T. S. Bates, J. A. Ogren, E. Andrews, and G. E. Shaw (2002), A 3-year record of simultaneously measured aerosol chemical and optical properties at Barrow, Alaska, *J. Geophys. Res.*, *107*(D11), 4130, doi:10.1029/2001JD001248.

Quinn, P. K., G. E. Shaw, E. Andrews, E. G. Dutton, T. Ruoho-Airola, and S. L. Gong (2007), Arctic haze: Current trends and knowledge gaps, *Tellus B*, *59*, 99–114.

Sahu, L. K., Y. Kondo, Y. Miyazaki, N. T. Kim Oanh, and P. Pongkiatkul (2011), Seasonal and diurnal variations of black carbon and organic carbon aerosols in Bangkok, *J. Geophys. Res.*, *116*, D15302, doi:10.1029/2010JD015563.

Sahu, L. K., et al. (2012), Emission characteristics of black carbon in anthropogenic and biomass burning plumes over California during ARCTAS-CARB 2008, *J. Geophys. Res.*, *117*, D16302, doi:10.1029/2011JD017401.

Sand, M., T. K. Berntsen, K. von Salzen, M. G. Flanner, J. Langner, and D. G. Victor (2016), Response of Arctic temperature to changes in emissions of short-lived climate forcers, *Nat. Clim. Change*, *6*, 286–289.

Schwarz, J. P., et al. (2006), Single-particle measurement of mid latitude black carbon and light-scattering aerosols from the boundary layer to the lower stratosphere, *J. Geophys. Res.*, *111*, D16207, doi:10.1029/2006JD007076.

Schwarz, J. P., R. S. Gao, A. E. Perring, J. R. Spackman, and D. W. Fahey (2013), Black carbon aerosol size in snow, *Sci. Rep.*, *3*, 1356, doi:10.1038/srep01356.

Sharma, S., J. R. Brook, H. Cachier, J. Chow, A. Gaudenzi, and G. Lu (2002), Light absorption and thermal measurements of black carbon in different regions of Canada, *J. Geophys. Res.*, *107*(D24), 4771, doi:10.1029/2002JD002496.

Sharma, S., M. Ishizawa, D. Chan, D. Lavoué, E. Andrews, K. Eleftheriadis, and S. Maksyutov (2013), 16-year simulation of Arctic black carbon: Transport, source contribution, and sensitivity analysis on deposition, *J. Geophys. Res. Atmos.*, *118*, 943–964, doi:10.1029/2012JD017774.

Sheridan, P. J., D. J. Delene, and J. A. Ogren (2001), Four years of continuous surface aerosol measurements from the department of energy's atmospheric radiation measurement program southern great plains cloud and radiation testbed site, *J. Geophys. Res.*, *106*, 20,735–20,747, doi:10.1029/2001JD000785.

Sherman, J. P., P. J. Sheridan, J. A. Ogren, E. Andrews, D. Hageman, L. Schmeisser, A. Jefferson, and S. Sharma (2015), A multi-year study of lower tropospheric aerosol variability and systematic relationships from four North American regions, *Atmos. Chem. Phys.*, *15*, 12,487–12,517.

Shindell, D., and G. Faluvegi (2009), Climate response to regional radiative forcing during the twentieth century, *Nat. Geosci.*, *2*, 294–300.

Shiraiwa, M., Y. Kondo, T. Iwamoto, and K. Kita (2010), Amplification of light absorption of black carbon by organic coating, *Aerosol Sci. Tech.*, *44*, 46–54.

Spackman, J. R., et al. (2010), Aircraft observations of enhancement and depletion of black carbon mass in the springtime Arctic, *Atmos. Chem. Phys.*, *10*, 9667–9680.

Verma, R. L., et al. (2011), Seasonal variations of the transport of black carbon and carbon monoxide from the Asian continent to the western Pacific in the boundary layer, *J. Geophys. Res.*, *116*, D21307, doi:10.1029/2011JD015830.

Warneke, C., et al. (2009), Biomass burning in Siberia and Kazakhstan as an important source for haze over the Alaskan Arctic in April 2008, *Geophys. Res. Lett.*, *36*, L02813, doi:10.1029/2008GL036194.

Warneke, C., et al. (2010), An important contribution to springtime Arctic aerosol from biomass burning in Russia, *Geophys. Res. Lett.*, *37*, L01801, doi:10.1029/2009GL041816.